

## STATUS OF THESIS

Title of thesis 2 D Modelling of Overpressure in the West Baram Delta, Sarawak

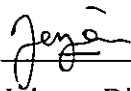
I JUHANA BINTI MISHAN hereby allow my thesis to be placed at the Information Resources Center (IRC) of Universiti Teknologi PETRONAS (UTP) with the following conditions:

1. The thesis becomes the property of UTP
2. The IRC of UTP may make copies of the thesis for academic purposes only.
3. This thesis is classified as

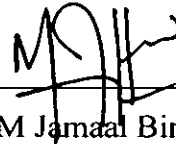
Confidential

Non-confidential

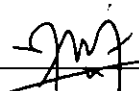
Endorsed by



\_\_\_\_\_  
Juhana Binti Mishan  
Kg.Pt. Hj. Salleh Khairun,  
Bt. 17 ¼, 86100 Ayer Hitam,  
Batu Pahat, Johor.  
Date: 02/01/2008



\_\_\_\_\_  
Dr. M Jamaal Bin Hoesni  
Level 4, Block C, PRSB,  
Kawasan Institusi Bangi,  
43000 Kajang,  
Selangor.  
Date: 02/01/08

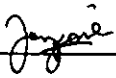


\_\_\_\_\_  
Dr. Azlina Binti Anuar  
Level 4, Block C, PRSB,  
Kawasan Institusi Bangi,  
43000 Kajang,  
Selangor.  
Date: 2 January 2008

UNIVERSITI TEKNOLOGI PETRONAS

Approval by Supervisors (s)

The undersigned certify that they have read, and recommend to The Postgraduate Studies Programme for acceptance, a thesis entitled "2D Modelling of Overpressure in the West Baram Delta, Sarawak" submitted by Juhana Binti Mishan for the fulfillment of the requirements for the degree of Master of Science in Petroleum Geoscience.



Date 02/01/2008

Signature

:



Main Supervisor

:

M. Jamaal Hoosni

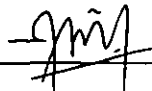
Date

:

02 Jan, 2008

Co-Supervisor 1

:

 (Aslina Amran)

**TITLE PAGE**

**UNIVERSITI TEKNOLOGI PETRONAS**

**2 D Modelling of Overpressure in the West Baram Delta, Sarawak**

**By**

**Juhana Binti Mishan**

**A THESIS**

**SUBMITTED TO THE POSTGRADUATE STUDIES PROGRAMME  
AS A REQUIREMENT FOR THE  
DEGREE OF MASTER OF SCIENCE IN PETROLEUM GEOSCIENCE  
PETROLEUM GEOSCIENCE  
BANDAR SERI ISKANDAR,  
PERAK.  
JANUARY, 2008**

I hereby declare that the thesis is based on my original work except for quotations and citations which have been duly acknowledged. I also declare that it has been previously or currently submitted for any other degree at UTP or other institutions.

Signature: Juhana

Name : Juhana Binti Mishan

Date : 02/01/2008

## ABSTRACT

This project is entitled 2D modeling of overpressure in the West Baram Delta, Sarawak, and the focus is on the basin study, reservoir fluid pressure, petroleum system and geophysical method. The main objective for this project is to reconstruct overpressure history in West Baram Delta area, with the aid of basin modelling. The study carried out in two phases. In the first phase, model reconstruction was based on disequilibrium compaction as the overpressuring mechanism. In the second phase, additional contribution to the development of overpressure from hydrocarbon generation was investigated. The methodology employed in this study include: seismic time to depth conversion, 1D modelling, pore pressure estimation and 2D Basin modelling. Based on seismic interpretation, the tectonics in the Baram Delta is shown very active as where many growth faults can be seen. This high tectonism in Baram Delta leads to shale diapirism. From 1D modelling the modeled basal heat flow range from  $25 \text{ mW/m}^2$  to  $53 \text{ mW/m}^2$ . The comparison of top overpressure suggest that in Well H is shallower, located at the depth of 1000 m, while the top of overpressure in Well O is at 1800 m. The 2D models have been calibrated with the observed pressure, temperature and vitrinite reflectance datasets.

The calibrated heat flow for the 2D modelling ranges from  $35 \text{ mW/m}^2$  to  $53 \text{ mW/m}^2$ . From the modeled overpressure in 2D basin modelling, the onset of overpressure is estimated to occur at 3050 m. In Well P, the top of overpressure was occurs at 3048 m, in Well A4 the depth occurs at 3100 m, Well O at 2987 m and Well H at 2682 m. In the first model of 2D basin modeling, the disequilibrium compaction indicates that overpressure starts approximately at 3050 m. In the second model, which includes the hydrocarbon generation, the depth of overpressure does not seem to vary much from the first model. It is therefore concluded that the main origin of overpressure in the West Baram Delta is disequilibrium compaction. Hydrocarbon generation does not contribute significantly to the development of overpressure in the Baram Delta.

## ACKNOWLEDGEMENT

In the process of completing this study, many individuals had helped me. Therefore, I would like to express my gratitude to the individuals that helped me a lot. Firstly, I wanted to say thank you to my supervisor Dr. M Jamaal Hoesni and my co-supervisor, Dr. Azlina Anuar for the valuable guidance and advices. Both of them are really dedicated and very helpful in guiding me throughout this study. Also thank you to En. Razali Che Kob for the lessons in seismic interpretation. I would also like to thank my friends, Azwa jannah Abu bakar for helping me to understand Drillworks Predict software and Mohammad Faizal Idris for helping me in seismic interpretation. Not to forget my thank you to Noorfarahida Ahmad Shariff and Wan Edani Wan Rashid for being so helpful throughout the process in completing my study. Also my thanks to my master programme classmates, my friends, Nur Aishah Hamir, Sity Arasy Mohd Yusak, Jarlin Santih, Hani Suraya Salim and Norhayati Abu Bakar for the support that they give me throughout this study. I really appreciate your moral support. To my family, especially my mother and father thank you so much for your tremendous support and understanding during this period of time.

## TABLE OF CONTENTS

Abstract	i
Acknowledgements	ii
Table of Contents	iii
List of Tables	v
List of Figures	vi

### CHAPTER ONE: INTRODUCTION

1.0	Introduction	1
1.1	Problem Statement	1
1.2	Objective	2
1.3	Scope of work	2
1.4	Overpressure: Concept and Terminology	2
	1.4.1    Disequilibrium Compaction	4
	1.4.2    Hydrocarbon Generation	5

### CHAPTER TWO: STUDY AREA

2.0	Study Area	6
2.1	Regional Geology of the Baram Delta	7
2.2	Structural Geology	9
2.3	Hydrocarbon System	9
2.4	Overpressure Distribution in the Baram Delta	10

### CHAPTER THREE: METHODOLOGY

3.0	Methodology and Data	12
3.1	Data	12
3.2	Seismic Interpretation (Seiswork)	15
3.3	1D Modeling (Genex)	17
3.4	Pore Pressure Estimation Using Drillworks Predict	19
3.5	Depth conversion (EasyDepth)	22
3.6	2 D Basin Modeling (Temis 2 D)	22

**CHAPTER FOUR: RESULTS AND DISCUSSION**

<b>4.0</b>	<b>Results and Discussions</b>	<b>24</b>
4.1	Seismic Interpretations (Seiswork)	24
4.2	Genex 1D Modeling (Genex)	28
4.3	Pore Pressure Estimation	42
4.4	Depth Conversion (Easydepth)	46
4.5	2 D Basin Modelling (Temis 2D) - Overpressure Origins	47
4.5.1	Disequilibrium Compaction Model	49
4.5.2	Hydrocarbon Generation Model	55

**CHAPTER FIVE**

<b>5.0</b>	<b>Conclusions and Recommendations</b>	<b>57</b>
------------	--	-----------

<b>REFERENCES</b>	<b>59</b>
-------------------	-----------

**APPENDICES**

<b>Appendix 1</b>	<b>64</b>
-------------------	-----------



**LIST OF TABLES**

<b>No.Tables</b>		<b>Pages</b>
Table 2.1	The top of overpressure observed in selected Baram Data wells (Abdul Jalil Muhammad & Azlina Anuar, 1999).	11
Table 3.1	Summary of data availability	14
Table 3.2	The available seismic line in the West Baram Delta.	15
Table 3.3	Interpreted horizons.	16
Table 4.1	Interpreted horizon for line 96SKE-030M.	24
Table 4.2	Interpreted horizon for line CW 98-096.	24
Table 4.3	Interpreted horizon for line CSK2K-04A.	24
Table 4.4	Selected well for 1D modelling.	39
Table 4.5	The depth of overpressure from the model and from report.	54

## LIST OF FIGURES

<b>Figures</b>		<b>Pages</b>
Fig.1.1	Pressure vs. depth plot. Rocks with pressures plotting above hydrostatic line and pore pressure line are overpressured; rocks with pressures plotting below the hydrostatic line are underpressured (adapted from Swarbrick & Osborne, 1998).	3
Fig.1.2	Overpressure generating mechanisms adapted from Swarbrick and Osbourne (1998).	4
Fig.1.3	Estimation of volume change when Type II kerogen in the Bakken shale, Williston Basin, matures to produce oil then wet gas and condensate, and finally dry gas. Note the increase in volume at all stages of thermal maturity of the kerogen (after Meissner, 1978b).	5
Fig.2.1	Map of Northern Borneo showing location of Baram Basin. Crocker Rajang accretionary complex and the northwest Borneo active margin (Expressed in the present day by the outer zone of thrusting and the northwest Borneo trough) (adapted from Tingay et. al., 2002).	6
Fig.2.2	Sedimentary basin and structural-stratigraphic provinces of the northern and eastern continental margins of Sarawak and Sabah. (After Mazlan B.Hj Madon, 1999).	7
Fig.2.3	Schematic geological cross section across the Baram Basin (Adapted from Koopman and James (1996a and b). The delta hinterland has been uplifted and eroded (Tingay et. al., 2002).	8
Fig.2.4	Growth faults are downthrown basin wards to the north and	9

northwest. (After Mazlan B. Hj. Madon, 1999).

- |          |   |    |
|----------|---|----|
| Fig.2.5  | The distribution of overpressure in the Baram Delta. From proximal to distal, the top of overpressure occurs deeper. This is related to the sedimentations rates. The sedimentation rates in the proximal is higher, thus the depth to overpressure depth in this area is shallower. The depth to overpressure in the distal area is deeper due to low sedimentation rates. (Adapted from Mazlan B. Hj. Madon, 1999). | 11 |
| Fig.3.1  | The workflow for this study includes data gathering, seismic interpretation, 1D modeling, pore pressure estimation, depth conversion and 2D Basin modeling.   | 12 |
| Fig. 3.2 | Selected wells for 1D modeling and oil/gas field distribution.  | 13 |
| Fig 3.3  | The three lines that were selected for seismic interpretations  | 14 |
| Fig.3.4  | Workflow method for seismic interpretation.   | 16 |
| Fig.3.5  | An example of a calibrated 1D model with temperature. The heat flow use is 54 mW/m <sup>2</sup> .   | 18 |
| Fig.3.6  | An example of a calibrated 1D model with the vitrinite reflectance. The heat flow used is 54 mW/m <sup>2</sup> . There are four points of VRo measurements that are not well calibrated. The past temperature indicated by the vitrinite reflectance was higher in the past, this is possibly due to the higher temperature sample from other vicinities which had been eroded and redeposited in this area.          | 18 |
| Fig.3.7  | Workflow for 1D Genex.  | 19 |

Fig.3.8	The relationship between the overburden pressure, pore pressure and the effective stress.	20
Fig.3.9	Flow chart of pore pressure estimation in Drillworks Predict.	21
Fig.3.10	Flow chart of conversion seismic time section to seismic depth section.	22
Fig.3.11	Flow chart methodology of basin modeling (Temis 2D)	23
Fig.4.1	Seismic Line 96SKE-030.	25
Fig.4.2	Seismic line CSK2K-04A.	26
Fig.4.3	Seismic line CW 98-096.	27
Fig.4.4	The temperature in Well D is well calibrated with the temperature.	29
Fig.4.5	The vitrinite reflectance is not well calibrated. The vitrinite reflectance value indicates a lower heat flow in the past, possibly due to vitrinite suppression, whereby the sample had been impregnated by oil.	29
Fig.4.6	The temperature in well A is quite well calibrated.	30
Fig.4.7	The vitrinite reflectance in Well A is suppressed.	30
Fig.4.8	The temperature in Well G is well calibrated.	31
Fig 4.9	The vitrinite reflectance in Well G is suppressed.	31
Fig.4.10	The temperature in well I is well calibrated.	32

Fig.4.11	The vitrinite reflectance in Well I is suppressed.	32
Fig.4.12	The temperature in Well H is well calibrated.	33
Fig.4.13	The vitrinite reflectance in Well H is suppressed.	33
Fig 4.14	The Temperature in Well F is Well calibrated.	34
Fig.4.15	The vitrinite reflectance in Well F is suppressed.	34
Fig.4.16	The temperature in Well J is well calibrated.	35
Fig.4.17	The vitrinite reflectance in Well J is suppressed.	35
Fig.4.18	In Well C, the temperature is well calibrated.	36
Fig.4.19	The vitrinite reflectance is not well calibrated in this well. The vitrinite reflectance indicated that the past temperature is higher than the temperature in present day. This is possibly due to vitrinite was recycling where the sample could have been eroded from another place that had higher past temperatures where redeposited in this area.	36
Fig.4.20	The temperature in Well B is well calibrated.	37
Fig.4.21	The vitrinite reflectance in Well B is eroded and recycled.	37
Fig.4.22	The temperature in Well E is well calibrated.	38
Fig.4.23	The vitrinite reflectance in Well E indicate the presence both eroded and recycled, and suppressed vitrinite.	38

Fig.4.24	Modeled heat flow distribution in the Baram Delta.	41
Fig.4.25	Well H and Well O for pore pressure estimation using Drillworks Predict.	42
Fig.4.26.	The overburden gradient trend for Well H and Well O.	43
Fig.4.27	The pore pressure estimation for Well H and Well O.	44
Fig.4.28	Comparison of pore pressure between Well O and Well H.	45
Fig.4.29	Interpreted horizons in time.	46
Fig.4.30	Velocity model after edited by layers and by patches.	46
Fig.4.31	Depth section – converted from seismic time section.	47
Fig.4.32	The lithology model for disequilibrium compaction.	47
Fig.4.33	Petrophysical data of the the lithology models.	48
Fig.4.34	Calibration for temperature in Well E – disequilibrium compaction.	49
Fig.4.35	The calibration of pressure in Well H.	50
Fig.4.36	The calibration of vitrinite reflectance in disequilibrium compaction model.	51
Fig.4.37	The vitrinite reflectance model.	52
Fig.4.38	The temperature model in present day for disequilibrium compaction.	53

Fig.4.39	The overpressure model for disequilibrium compaction.	54
Fig.4.40	The lithology model for hydrocarbon generation model.	55
Fig.4.41	West Baram major oil and gas fields (Adapted from Denis N. K. Tan et. al., 1999).	56
Fig.4.42	The hydrocarbon expulsion for hydrocarbon generation model - hydrocarbon expulsion model.	56

## CHAPTER ONE

### 1.0 Introduction

This project is entitled 2D modeling of overpressure in the West Baram Delta, Sarawak, and focused on the basin study, reservoir fluid pressure, petroleum system and geophysical method. 2D forward modeling will be applied to predict overpressure development due to disequilibrium compaction, as well as the possible contribution of overpressuring from hydrocarbon generation and oil-gas conversions.

### 1.1 Problem Statement

The West Baram Delta is Tertiary in age, which experienced the rapid deposition of thick low permeability sediments leading to the development of overpressure. The main overpressuring mechanism is disequilibrium compaction. In a recent study of the West Baram Delta, it was found that the interval pressure gradient at the onset of overpressure varies from shelfal to the deeper water areas. The study concluded that the variation is due to the sedimentation and tectonic histories. The active tectonisms in the area are reflected by the development of growth faulting and shale diapirism. This are closely associated with the overpressured shale (M Jamaal Bin Hoesni, 2004).

For this project, the number of well control and depth of penetration are limited. Poor seismic reflection made the prediction of the onset and the magnitude of overpressure problematic. Thus, forward basin modeling, which incorporates sediment compaction, hydrodynamic and thermal evolution, helped to improve the prediction of overpressure. Through basin modeling, other overpressuring mechanisms, such as volume expansion and lateral fluid transfer, can also be assessed.



## **1.2 Objectives**

The objective for this project is to reconstruct overpressure in The West Baram area, with aid of basin modelling:

In the first phase, model reconstruction will be based on disequilibrium compaction as the over pressuring mechanism.

In second phase, the additional contribution of hydrocarbon generation will be investigated.

## **1.3 Scope of Work**

To accomplish the objectives, this study will apply 2D forward modeling in predicting overpressure. Therefore this study aims to provide reliable prediction of pore pressure for drilling. Several softwares have been utilized, such as Seiswork for interpreting the seismic line, Genex for 1D modeling, Temis 2D for predicting overpressure due to disequilibrium and Drillworks Predict for estimating the pore pressure in the formation.

## **1.4 Overpressure : Concept and Terminology**

Overpressure is defined as when the amount of pore pressure exceeding the hydrostatic line (Dickinson, 1953). In order to understand more about overpressure, other terminologies such as hydrostatic pressure overburden and effective stress also need to be understood. Figure 1.1 is a diagram describing the terminologies related to overpressure.

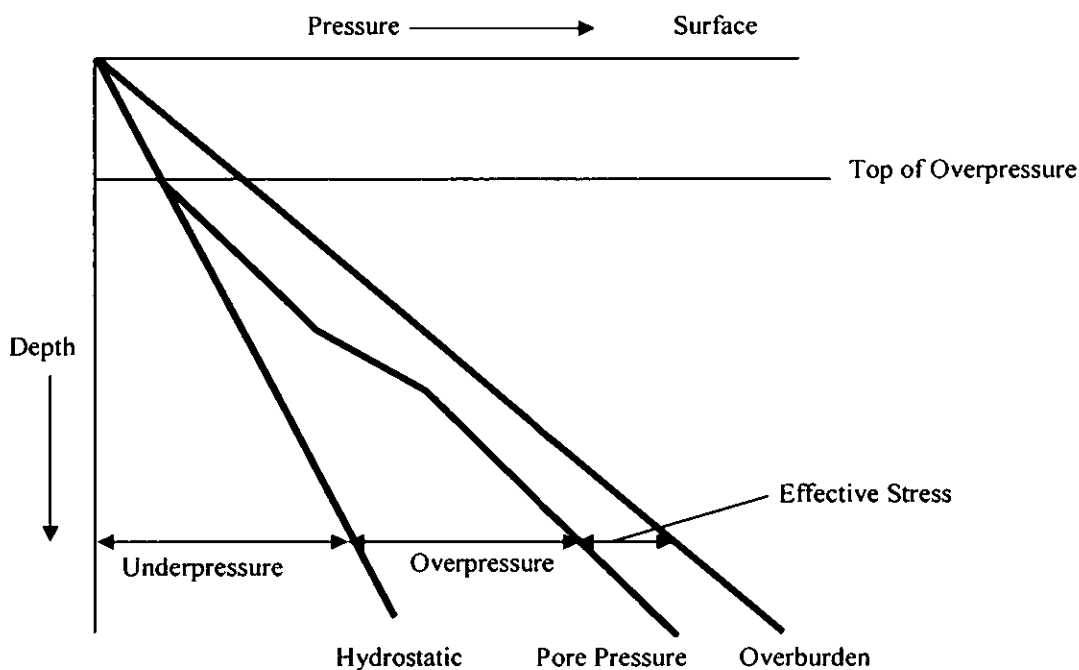


Fig. 1.1 Pressure vs. depth plot. Rocks with pressures plotting above hydrostatic line and pore pressure line are overpressured; rocks with pressures plotting below the hydrostatic line are underpressured (adapted from Swarbrick & Osborne, 1998).

Pore pressure is the pressure of the liquid in the pore space of the rock. As suggested in Figure 1.1, this can be higher than hydrostatic pressure. The point where the pore pressures exceed the hydrostatic pressure is the “top of overpressure” (Bruce, 2002). Overpressure also can be described, in terms of the dynamics of subsurface fluid flow, as the inability of formation fluids to escape at a rate which allows equilibrium with hydrostatic pressure. One of the primary controls on the presence and distribution of overpressure is permeability, the rock attribute which controls seal behavior (Swarbrick & Osborne, 1998). The hydrostatic pressure gradient varies from 0.433 psi/ft (9.71 kPa/m) for fresh water, to approximately 0.51 psi/ft (11.44 kPa/m) for saturated brine (Swarbrick & Osborne, 1998).

When the pore pressure is lower than the hydrostatic pressure, underpressure condition will occur. Usually, underpressure results from the depletion of oil and gas during production (Swarbrick & Osborne, 1998). Swarbrick and Osborne (1998) categorize the processes which lead to overpressure in to three categories (Figure 1.2).

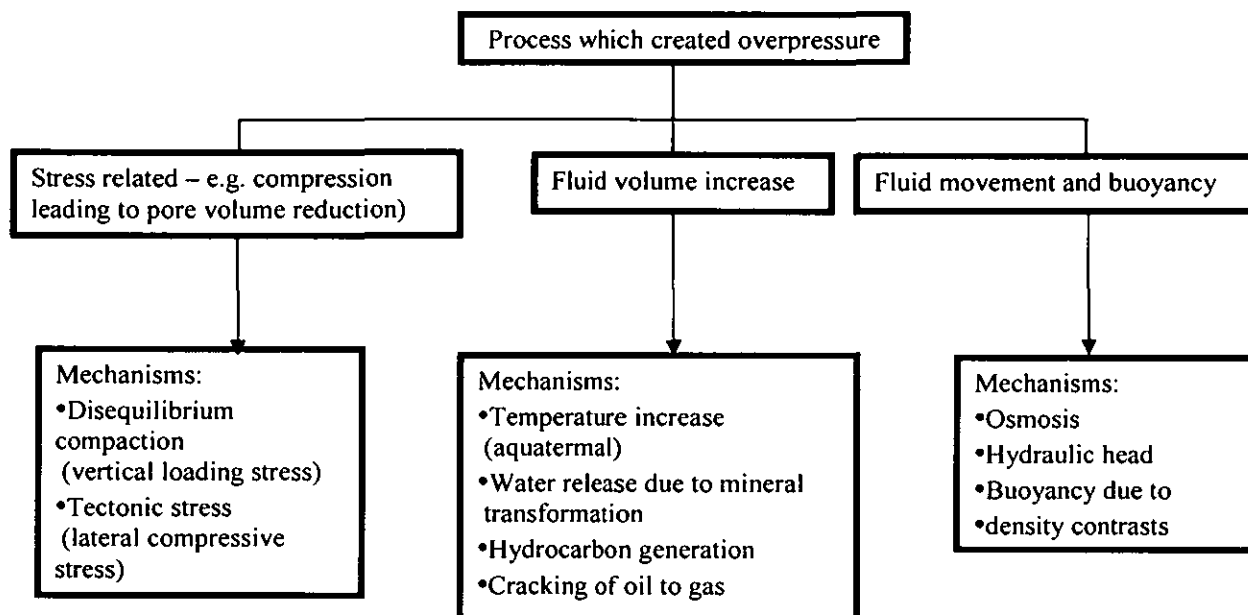


Fig. 1.2 Overpressure generating mechanisms adapted from Swarbrick and Osbourne (1998).

### 1.4.1 Disequilibrium Compaction

Disequilibrium compaction is defined as a condition where fluids cannot be expelled fast enough relative to sediment loading resulting the pressure of the pore fluids increase (Swarbrick & Osbourne, 1998). Terzaghi's (1923) lab experiment cited that, for disequilibrium compaction, anomalously high porosity estimates are observed in low permeability sections (Swarbrick & Osbourne, 1998).

During slow burials, the equilibrium between overburden stress and the reduction of pore fluid volume due to compaction can be most easily maintained. However, in fast burials, the liquid will not be able to escape due to rapid increase of overburden stress leading to their entrapment. This results in overpressure due to disequilibrium compaction. The overburden stress is also referred to as lithostatic stress and/or geostatic stress (Swarbrick & Osbourne, 1998).

### 1.4.2 Hydrocarbon Generation

The generation of liquid and gaseous hydrocarbons from kerogen maturation is kinetically controlled and dependent on time and temperature (Swarbrick and Osborne, 1998).

A study that involve hydrocarbon as the mechanism of overpressure is in Williston Basin, North Dakota, USA Meissner (1978 a). Meissner (1978b) cited that the abnormal pressure of the hydrocarbon generation is due to the increasing volume of hydrocarbon and residue relative to unaltered organic material (Figure 1.3). Another reason of the abnormal pressure is due to the remaining collapse of the rock framework as overburden-supporting solid organic matter is converted to hydrocarbon pore fluid. However, Swarbrick & Osborne (1998) believed that it is premature to assume that there is an overall fluid volume increase in all cases of kerogen – oil conversion.

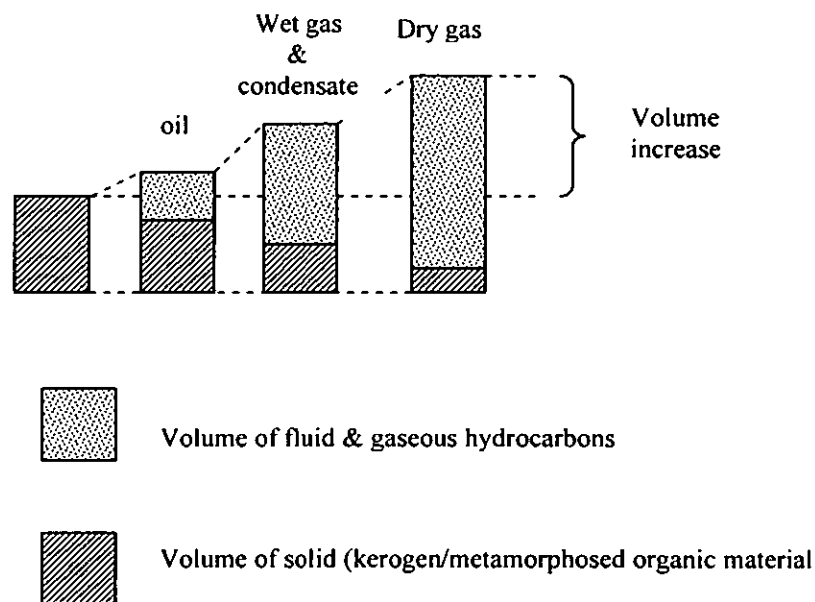


Fig. 1.3. Estimation of volume change when Type II kerogen in the Bakken shale, Williston Basin, matures to produce oil then wet gas and condensate, and finally dry gas. Note the increase in volume at all stages of thermal maturity of the kerogen (after Meissner, 1978b).

## CHAPTER TWO

### 2.0 Study Area

The study area is the West Baram Delta (Figure 2.1). Eventhough the Baram Delta is included in the Sarawak Basin, it is only a third of the total delta area (Figure 2.2). The remainder of the Baram Delta lies in Negara Brunei Darussalam and Sabah (Mazlan B. Hj Madon, 1999). Hence, the Baram Delta province of the Sabah Basin lies to the east of the West Baram line and which are characterized by lower geothermal gradients, and much higher post-Middle Miocene subsidence rates (Mazlan B. Hj. Madon, 1999 adapted from Noor Azim Ibrahim, 1994).

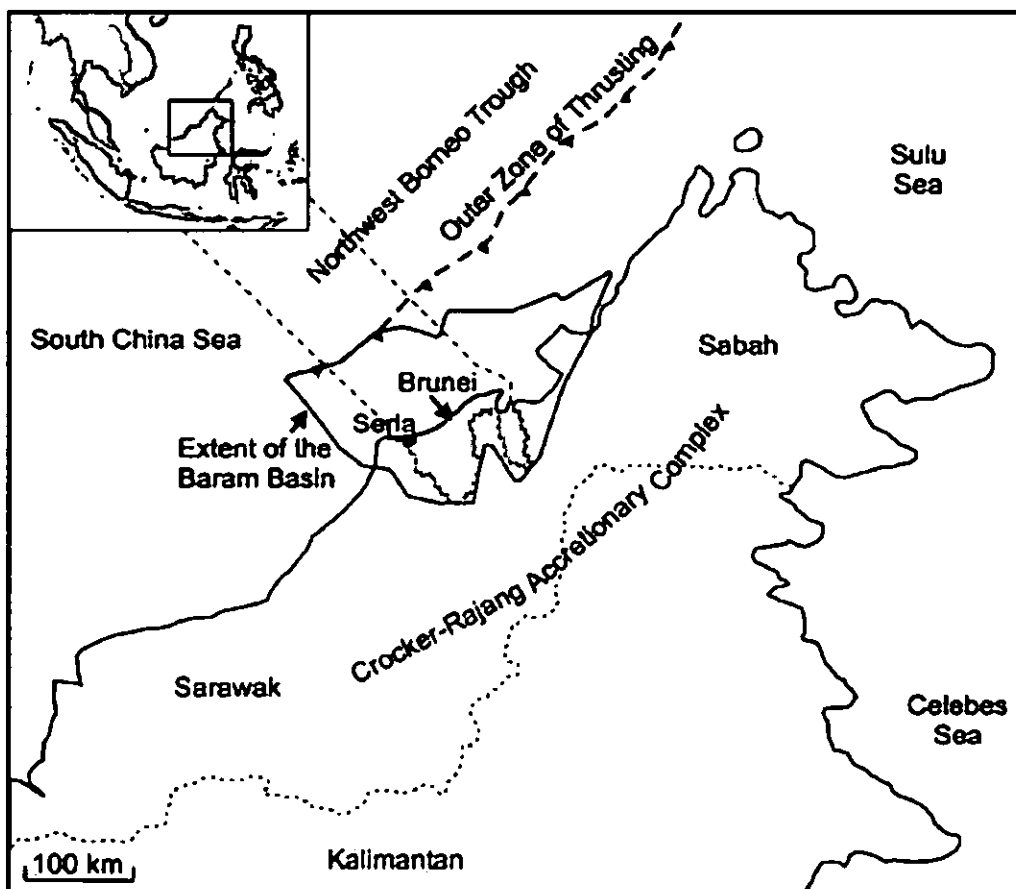


Fig 2.1. Map of Northern Borneo showing location of Baram Basin. Crocker Rajang accretionary complex and the northwest Borneo active margin (expressed in the present day by the outer zone of thrusting and the northwest Borneo trough) (adapted from Tingay et. al., 2002).

## 2.1 Regional Geology of the Baram Delta

The Baram Delta Province covers an area of 7500 km<sup>2</sup> including 2500 km<sup>2</sup> onshore (Mohammad Yamin Ali et. al., 1995). This province evolved during the Middle Miocene to present day from a foreland basin to a shelf margin (Morley et. al., 2002). The basin is perhaps best described as a peripheral foreland basin that formed after the collision of Reed Bank and Dangerous Grounds micro continental fragments with northwestern Sabah (Mazlan B. Hj. Madon, 1999). The Baram Delta depocentre developed during the early Miocene, probably as a fault-controlled depression formed at the intersection of two major crustal-scale faults, namely the West Baram Line to the west and the Jerudong-Morris fault to the east. This two major crustal scale basement appear to confine the Baram Delta Province Figure 2.2, (Mazlan B. Hj. Madon, 1999).

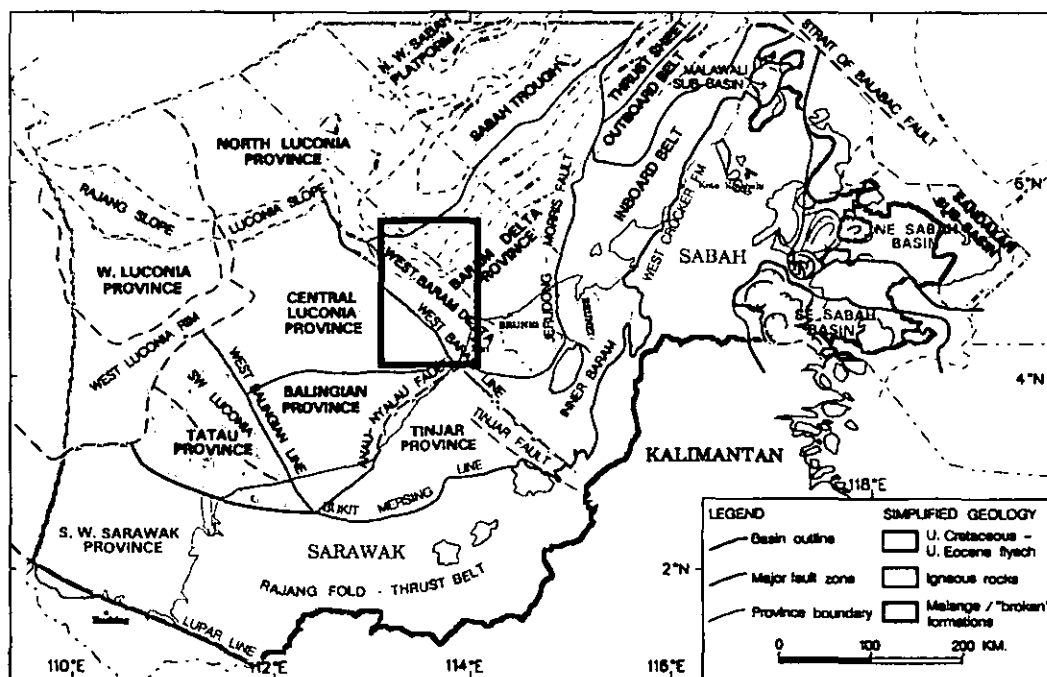


Fig. 2.2 Sedimentary basin and structural-stratigraphic provinces of the northern and eastern continental margins of Sarawak and Sabah. (After Mazlan B.Hj Madon, 1999).

This late Neogene Baram Basin is composed of several rapidly prograding delta systems built outwards from the Crocker–Rajang accretionary complex and deposited adjacent to the northwest Borneo active margin (Koopman & James, 1996a). The active tectonic setting has resulted in a complex interaction between sedimentation and tectonics in variable uplift of the hinterland, sediment reworking

and fast depositional rates (Tingay et. al., 2002). Transpressive deformation associated with the active margin has caused uplift in the proximal and the eastern part of the basin (Koopman & James, 1996b; Figure 2.3). The uplifted sediments were then eroded, reworked and deposited further down the delta (Tingay et. al., 2002). Episodic folding events affected the region, causing uplift of the hinterland, delta progradation and the inversion of gravity-related faults (Morley et. al., 2002).

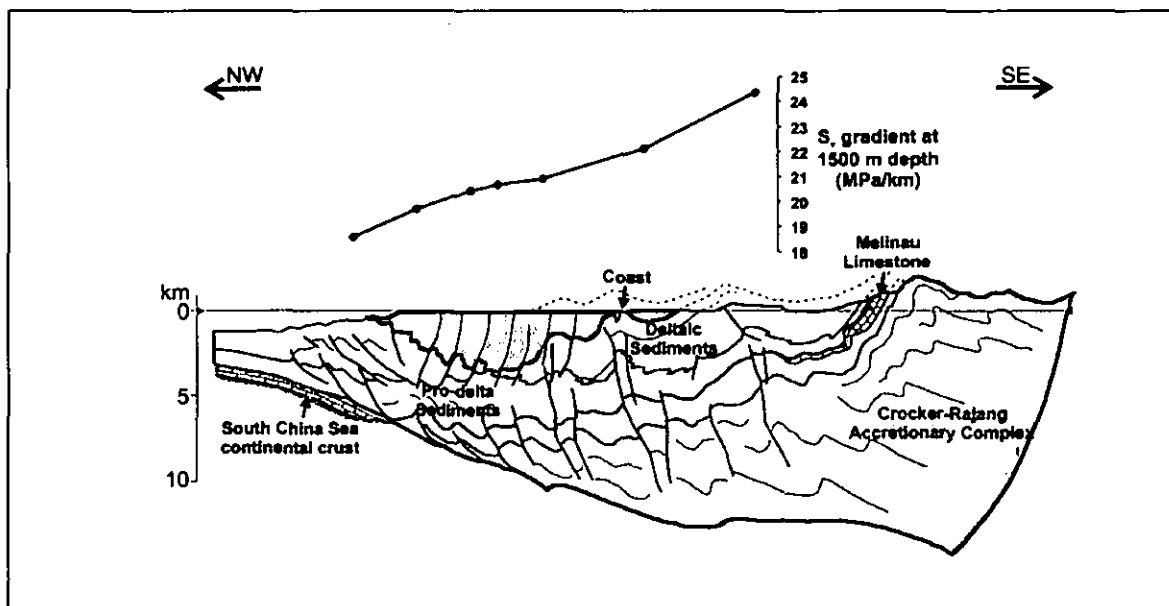


Fig. 2.3. Schematic geological cross section across the Baram Basin (adapted from Koopman and James (1996a and b). The delta hinterland has been uplifted and eroded (Tingay et. al. 2002).

The rapid deposition of fine-grained prodelta sediments led to the development of widespread overpressure generated by disequilibrium compaction (Schreurs & Ellenor, 1996). Overpressures within the prodelta shales are commonly associated with undercompaction and shale diapirism (Schreurs & Ellenor, 1996). Sedimentation in the Baram Delta started with a predominantly argillaceous sequence interbedded with limestones and minor sandstone until the middle Miocene (Mazlan B. Hj. Madon, 1999).

Reservoir sands occur mostly in Upper Miocene-Lower Pliocene Middle Cycle V- to Cycle VI topsets. Stacked rollover structures are present on the hanging wall of growth faults (Mazlan B. Hj. Madon, 1999). The prolific hydrocarbon province of the Baram Delta was formed in Middle Miocene-recent deltaic sedimentary rocks (Morley et. al., 2003).

## 2.2 Structural Geology

While many of the structural features are typical of gravity tectonics in large deltas such as growth faults, shale diapirs and toe thrusts (James, 1984; Sandal, 1996), the structures have been commonly modified by the growth of compressional or strike-slip related folds and thrusts (Bol and van Hoorn, 1980; James, 1984; Levell, 1987; Bait and Banda, 1994; Sandal, 1996; Morley et al., 1998).

Most large delta provinces described in the literature are developed on passive margins (e.g. the Mississippi, the Nile, the Niger Deltas) but the Baram Delta Province is different as it developed on a tectonically active margin (Morley et al., 2003). Another example of such a delta is the Kutei Basin of Eastern Borneo (Ferguson and McClay, 1997; McClay et al., 2000).

The structure of the Baram Delta Province is dominated by regional growth faults which are downthrown basinwards to the north and northwest (Figure 2.4).

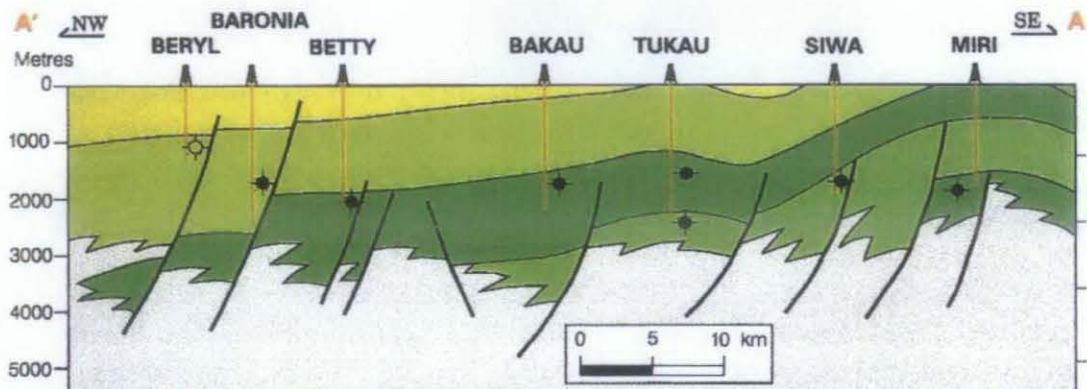


Fig. 2.4. Growth faults are downthrown basinwards to the north and northwest. (After Mazlan B. Hj. Madon, 1999).

## 2.3 Hydrocarbon System

The identification of source rock intervals in the Baram Delta Province is challenging as the organic matter is not abundant and appears to be concentrated within very thin layers (Mohammad Yamin Ali et al., 1995). Furthermore, the deepest well only penetrated Cycle IV sequences (Mohammad Yamin Ali et al., 1995). The higher land-plant debris transported into the West Baram Delta would



have been reasonably preserved by virtue of their rapid removal from the oxidation zones (Denis N.K Tan et. al., 1999). Today, it is accepted that the hydrocarbons in the West Baram Delta were generated mainly from transported terrigenous organic matter (Denis N.K Tan et. al., 1999). The terrigenous source for the Baram Delta oils was proven by Azlina Anuar & Abdul Jalil Muhamad (1999) through GCMSMS analysis.

Good reservoir characteristics were best developed during Cycles V to Cycle VI regressions. These reservoirs are mainly beach, coastal barrier and shallow neritic sheet sands deposited in deltaic coastal plain, coastal and fluviomarine environments (Mohammad Yamin Ali et. al., 1995)

The seals in this delta are the thick shale sequences. These shales are well developed very well during the Cycle VI deposition. Therefore, none of the hydrocarbon would be leaked out into the sequences younger than Cycle VI (Mohammad Yamin Ali et. al., 1995).

Fault-closed structures within the Cycle V sequences act as traps for the hydrocarbons. The main trapping mechanisms are the major growths faults (Mohammad Yamin Ali et. al., 1995).

Hydrocarbon migration occurred between 3.0 to 3.6 Ma when the amounts of overpressure decreased and hydrocarbon might expel and migrate into reservoir rocks, as suggested by Mohammad Yamin Ali et. al. (1995).

#### **2.4 Overpressure Distribution in the Baram Delta**

Table 2.1 shows previous study (Abdul Jalil Muhammad & Azlina Anuar, 1999) the depth to the top of overpressure seen in several wells. This overpressure is due to disequilibrium compaction. High sedimentation rates can be found in proximal part of the delta. In the hinterland, the sediments were uplifted and eroded and subsequently transported to the distal parts. From the data observed (Table 2.1), the trend of the overpressure is deeper in the distal area. While the depth of overpressure is shallower in the proximal area (Figure 2.5).

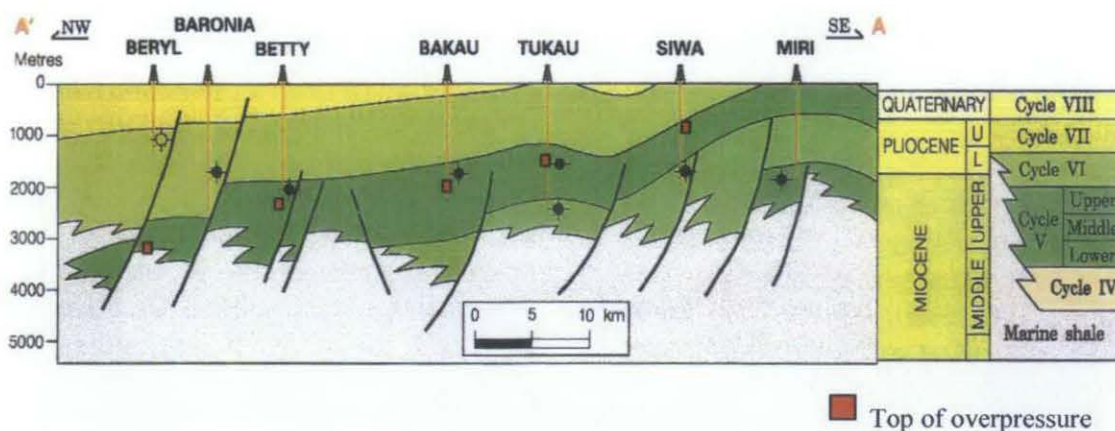


Fig. 2.5. The distribution of overpressure in the Baram Delta. From proximal to distal, the top of overpressure occurs deeper. This is related to the sedimentations rates. The sedimentation rates in the proximal is higher, thus the depth to overpressure depth in this area is shallower. The depth to overpressure in the distal area is deeper due to low sedimentation rates. (Adapted from Mazlan B. Hj. Madon, 1999)

Table 2.1. The top of overpressure observed in selected Baram Data wells (Abdul Jalil Muhammad & Azlina Anuar, 1999)

	Well name	Top of overpressure (m)
1	A5	2652
2	A6	2896
3	A7	2987
4	D	3272
5	A8	3444
6	A9	3063
7	G	3319
8	B1	3658
9	F	3048
10	B2	2305
11	H	2774
12	J	2225
13	A	1996

## CHAPTER THREE

### 3.0 Methodology and Data

Data for this study were derived from various sources such as from technical reports (final well reports, well test reports) or geochemical reports (from UDRS) and from Petronas Management Unit, (PMU). Figure 3.1 illustrates the workflow for this study.

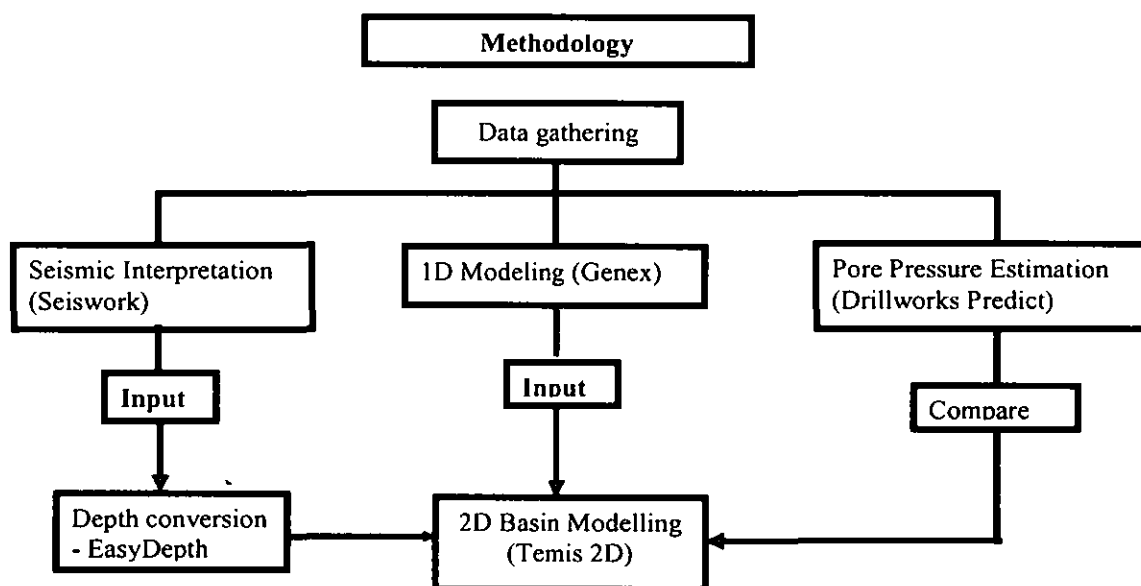


Fig. 3.1 The workflow for this study includes data gathering, seismic interpretation, 1D modeling, pore pressure estimation, depth conversion and 2D Basin modeling.

### 3.1 Data

The data needed for seismic interpretation are seismic sections to determine the horizons of Cycles VI, Middle Cycle VI, Lower Cycle VI, and Upper Cycle V. As for 1D basin modeling (Genex), the data needed are temperature and vitrinite reflectance; this data is gathered from geochemical report. For pore pressure estimation (Drillworks Predict) the data needed are ASCII Data of wireline logs, pressure data (mudweight, Repeat Formation Test (RFT), Leak off Test (LOT)). Below are the well data statistic (Table 3.1), from selected wells for 1D modeling (Figure 3.2) and seismic lines in SK307 (Table 3.2 and Figure 3.3).

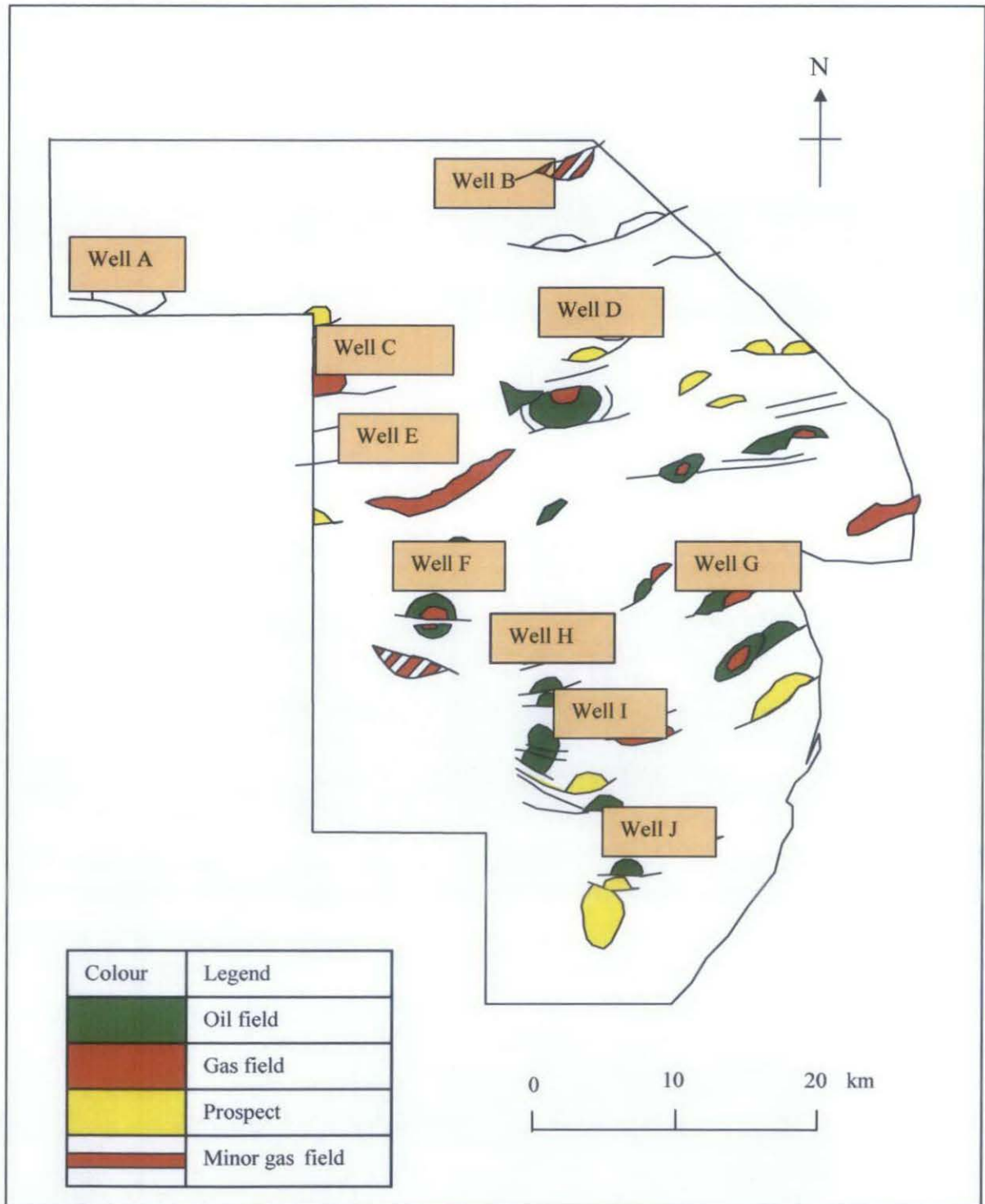


Fig. 3.2 Selected wells for 1D modeling and oil/gas field distribution.

Table 3.1. Summary of data availability.

Data	Availability
Numbers of wells	135 wells
Geochemistry data	26 reports
Wireline logs	57 logs
Pressure	54 reports
Temperature	11 reports

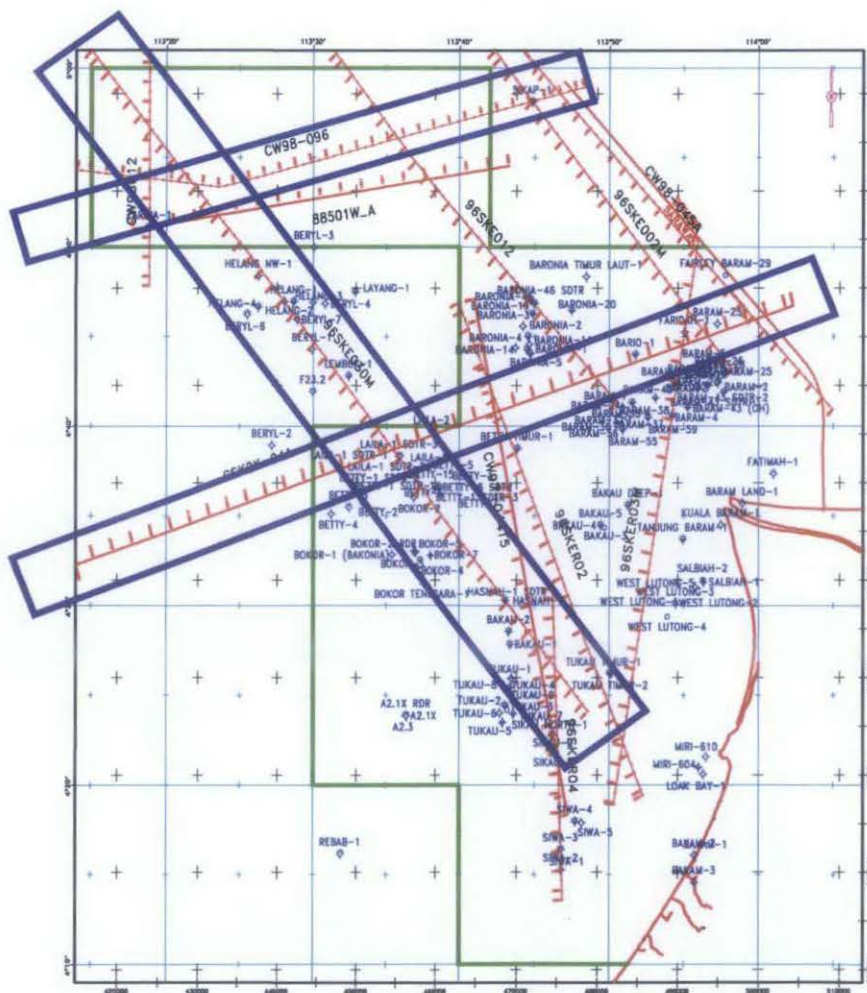


Fig 3.3. The three lines that were selected for seismic interpretations.

Table 3.2 The available seismic line in the West Baram Delta.

	Seismic line No.	Wells located on the seismic line	Interpreted line
1	88-501W	A	
2	96SKE-002M	K	
3	96SKE-012	L, M	
4	96SKE-030M	H, O, P, A4	√
5	96SKE-02	Q, R	
6	96SKER-03M	S, T, U	
7	96SKER-04	V, W, X, Y	
8	CW97-044	Z	
9	CW97-045A	A1	
10	CW98- 096	B	√
11	SK2K-04A	A2, A3	√

### 3.2 Seismic Interpretation (Seiswork)

The interpreted seismic line, 96SKE-030M, is used as input for the Temis 2D modeling. There are four (4) wells located on the seismic line, namely H, O, P and A4. However, two wells (Well H and well O) available in digital format logs, so this two wells were chosen as the control wells and used for horizon picking. As for well A4, there are no composite logs that provide the depth of the cycles. As for well P, there is no wireline curve provided in the workstation database. The interpreted horizons are the top horizon Cycle VI, Cycle VI Middle, Lower Cycle VI, top of Cycle V, middle of Cycle V, (Table 3.3). There were some difficulties in interpreting the NE part of the seismic line. This part is near to the deep water area where the seismic reflection is poor and unclear. Other interpreted lines are CW 98-096 and CSK2K-04A. The control well for line CSK-04A is Well A3 and the control well for CW 98-096 is Well B.

In order to determine and to identify the horizons of the Top Cycle VI, Middle Cycle VI, Lower Cycle VI, Top Cycle V and Lower Cycle V, the two way time (TWT) vs. depth graph is used. This data is obtained from check shot data that are available in the workstation database. The depth of Cycles from Top Cycle VI to Middle Cycle V can be obtained from the composite logs in final well report. Since

the information of the cycles in the composite logs is in depth and not in time, the time vs. depth graph is used to determine the time of each cycles. After the time of each cycle has been identified, interpretations of the cycles were proceed. Selected horizons were interpreted with the major faults also interpreted. The major faults were identified by the present displacement along the horizons. Figure 3.4 show the workflow for seismic interpretation.

Table 3.3. Interpreted horizons.

Cycle (horizon)	Age	Ma
Top Cycle VI	Late Pliocene	3.0
Middle Cycle VI	Middle Pliocene	3.8
Lower Cycle VI	Early Pliocene	4.2
Top Cycle V	Late Miocene	5.6
Middle Cycle V	Middle Late Miocene	6.7

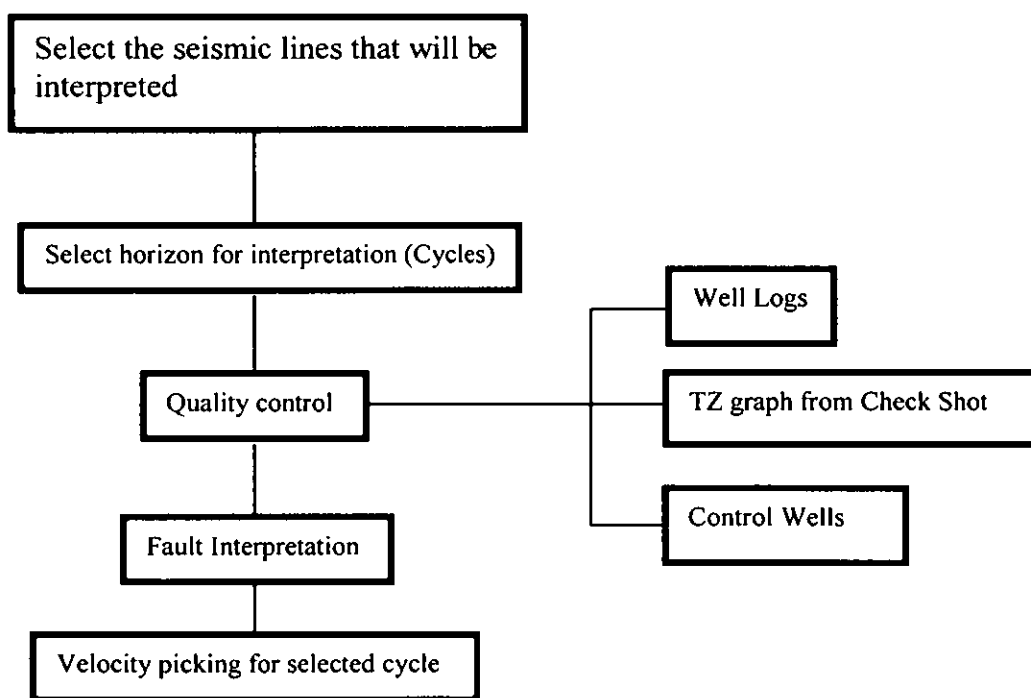


Fig. 3.4 Workflow method for seismic interpretation.

### 3.3 1D Modeling (Genex)

The purpose of 1D modeling is to reconstruct the past thermal history of the basin based on the well data. The required data for 1D modeling are temperature, vitrinite reflectance (VRo), and well lithology. The temperature data obtained for the 1D modeling are from production tests, such as Repeat Formations Tests (RFT). These tests provide the present day temperature and the present day heat flow. Vitrinite reflectance (VRo), represents the past temperature history and also the past heat flows. These two (2) different heat flows, the past and the present will have their own significances in calibrating the temperature and the vitrinite reflectance. In certain cases, the heat flow is different from the past and the present day, making the calibration more difficult.

However, calibration is crucial in reconstructing the past history of the basin; therefore, temperature data and vitrinite reflectance (VRo) data are essential. If both data calibrate, then the result of the 1D modeling is reliable. The result obtained from 1D modeling is the heat flow. However, in this study, there are several wells where heat flows do not calibrate with vitrinite reflectance. This will be discussed in the Results and Discussion section. Below is an example of the 1D modeling that calibrated reasonably well with temperature and vitrinite reflectance data (Figure 3.5 & 3.6).

The selection of the well for 1D modeling is based on the availability of the temperature data and vitrinite reflection (VRo). The selection of wells was also based on the location of the wells. The locations of the wells represent area from the proximal to the distal. This is to see whether there is a certain trend of the heat flow from proximal to distal. Figure 3.7 shows the workflow of 1 D modeling.



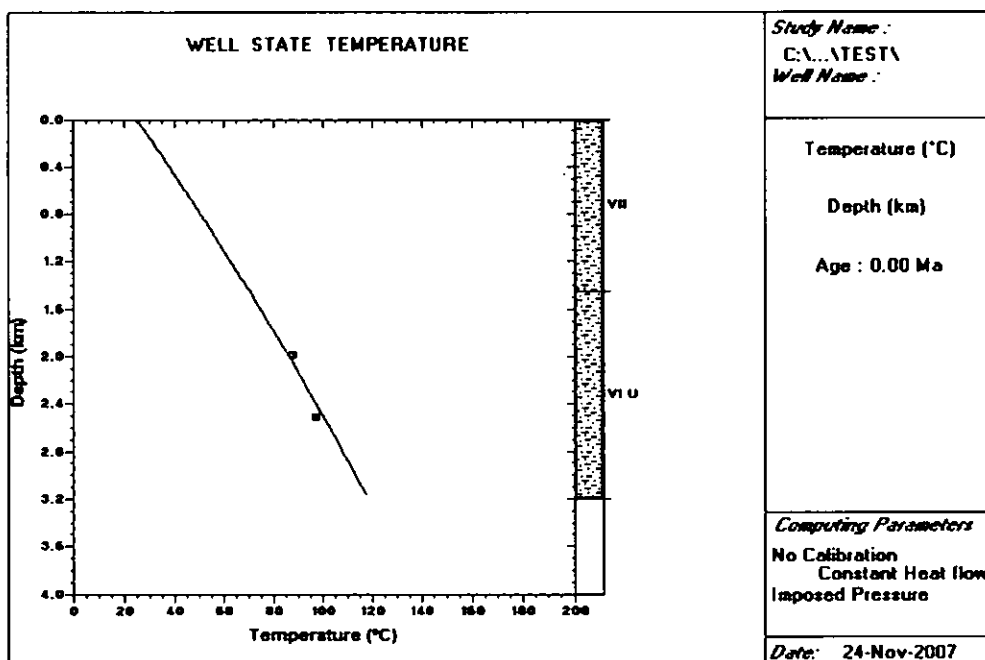


Fig. 3.5. An example of a calibrated 1D model with temperature. The heat flow use is  $54 \text{ mW/m}^2$

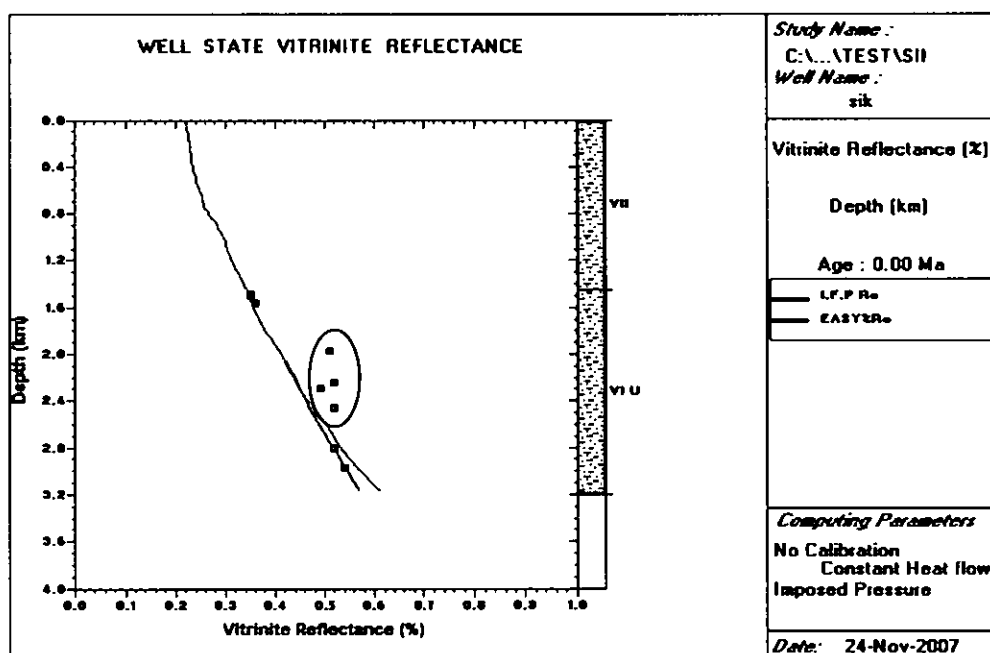


Fig.3.6. An example of a calibrated 1D model with the vitrinite reflectance. The heat flow used is  $54 \text{ mW/m}^2$ . There are four points of VRo measurements that are not well calibrated. The past temperature indicated by the vitrinite reflectance was higher in the past, this is possibly due to the higher temperature sample from other vicinities which had been eroded and redeposited in this area.

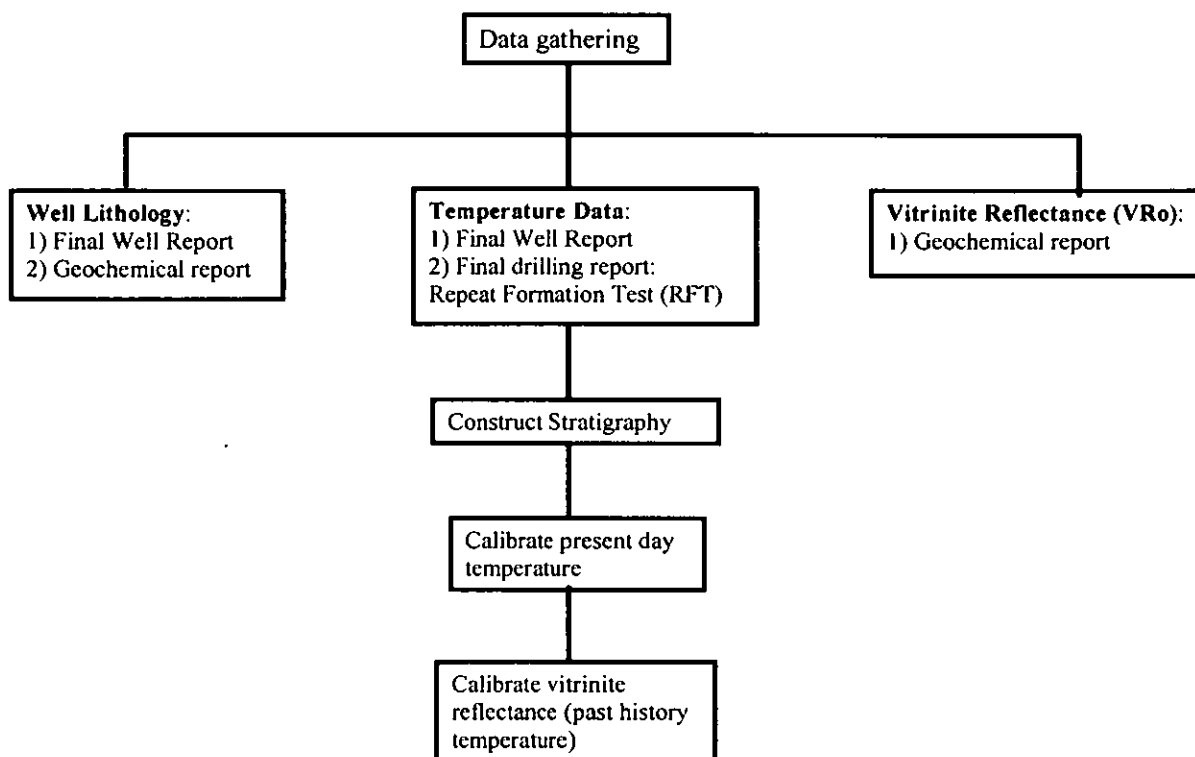


Fig. 3.7. Workflow for 1D Genex.

### 3.4 Pore Pressure Estimation Using Drillworks Predict

For the pore pressure estimation, two wells (Well H and Well O) were selected. The wells were selected as they are located on the modeled section seismic line. There are several methods in estimating the pore pressure (Drillworks Pro Training Course, 2005). The five methods are:

- 1) Velocity /effective stress relationship
- 2) Horizontal and vertical methods
- 3) Eaton's equations
- 4) Bower's methods
- 5) Miller's Method

In this study, Eaton's method was applied in estimating the pore pressure. The basic relationship between total vertical stress or overburden, effective vertical stress (rock or matrix stress) and formation fluid pressure (pore pressure), (Figure 3.8) was explained by Terzaghi, using the equation below:

$$S_v = \sigma_e + P_f$$

$S_v$  = Total vertical stress/ overburden

$\sigma_e$  = Effective vertical stress (Rock or Matrix stress)

$P_f$  = Formation fluid pressure (pore pressure)

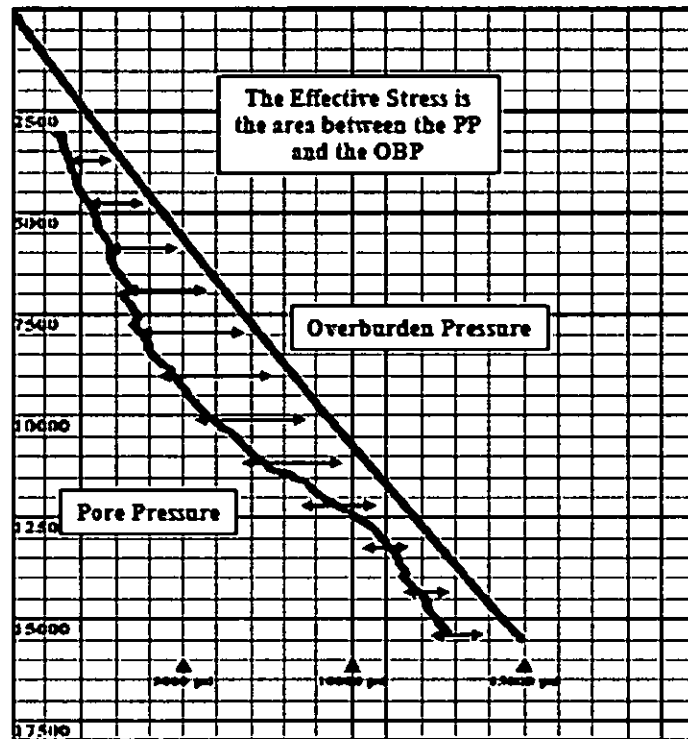


Fig. 3.8. The relationship between the overburden pressure, pore pressure and the effective stress. (Drillworks ProTraining Course, 2005).

Below is the flow chart for estimating pore pressure by Drillworks Predict (Figure 3.9).

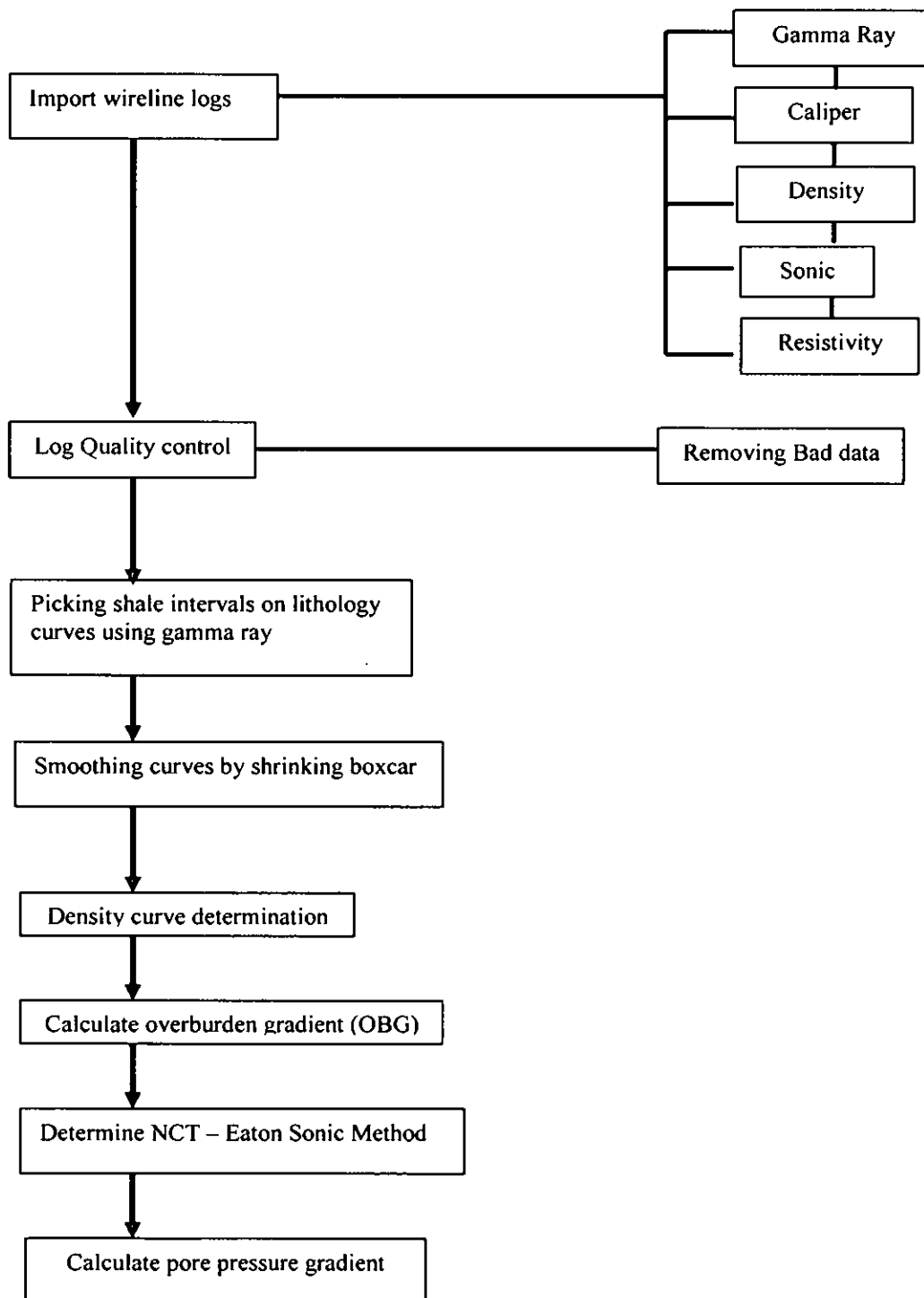


Fig.3.9. Flow chart of pore pressure estimation in Drillworks Predict.

### 3.5 Depth Conversion (EasyDepth)

In order to construct the modeling, firstly, the seismic time section need to be converted to seismic depth section, to do this, software called Easydepth was utilized. Figure 3.10 shows the workflow of the conversion seismic time section to seismic in depth section.

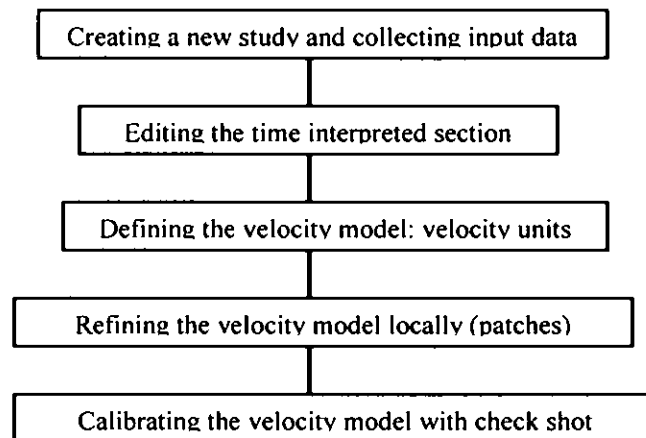


Fig. 3.10. Flow chart of conversion seismic time section to seismic depth section.

### 3.6 2D Basin Modelling (Temis 2D)

After converting the time seismic section to depth seismic section, the section can then be exported to Temis 2D for constructing the model. Below are steps of the method to run the simulations. Figure 3.11 shows the workflow of 2D basin modelling.

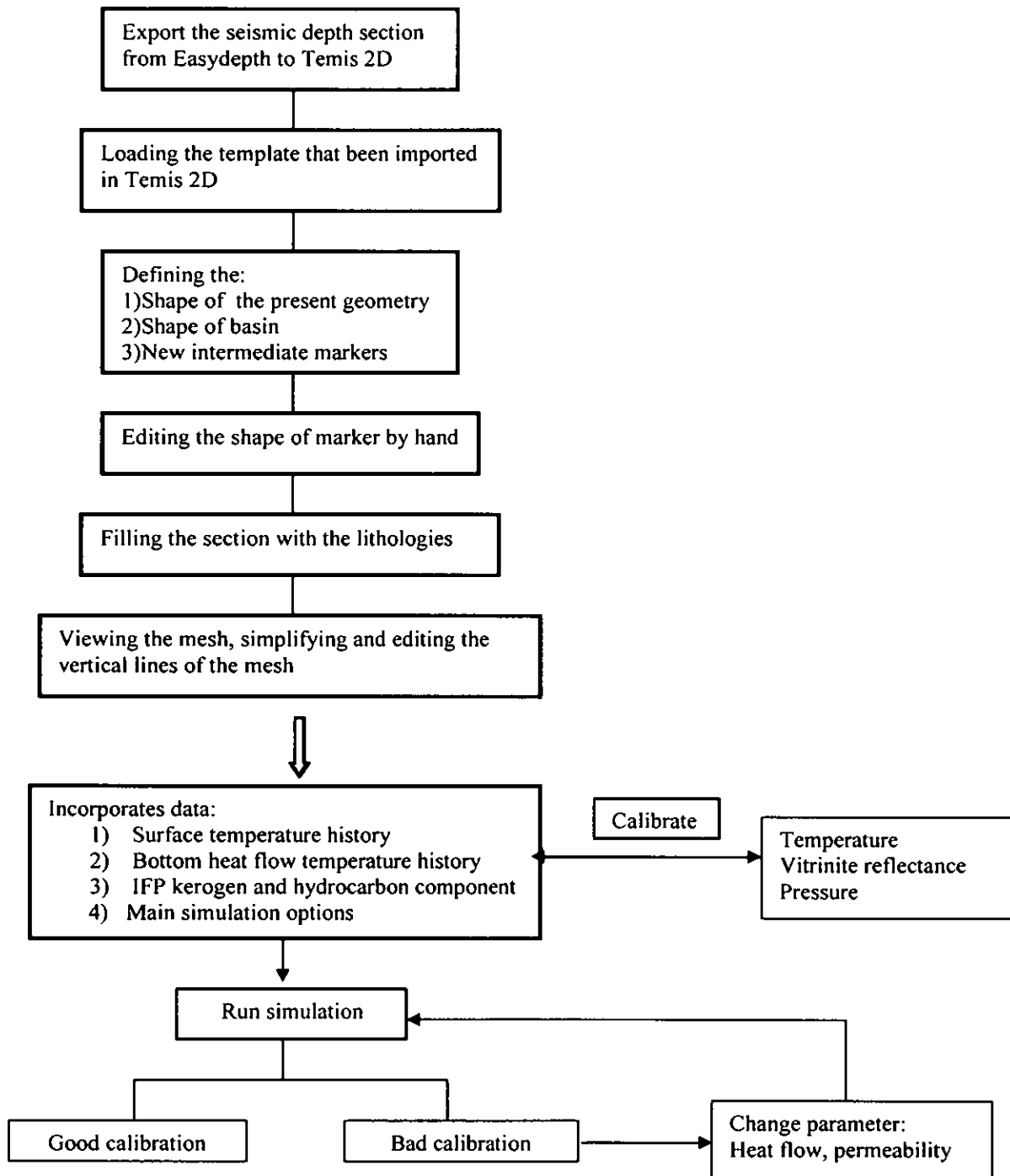


Fig. 3.11 Flow chart methodology of basin modeling (Temis 2D)

## CHAPTER FOUR

### 4.0 Results and Discussions

Results and discussion for seismic interpretations, 1D modeling, and pore pressure estimation are as below.

#### 4.1 Seismic Interpretations (Seiswork)

Five horizons were interpreted, and the interpreted horizons are as below (Table 4.1, table 4.2, table 4.3) and (Figure 4.1, 4.2, 4.3).

Table 4.1. Interpreted horizon for line 96SKE-030M.

horizons	interpretations	Well H	Well O	Well P	Well A4
Top Cycle VI	√	320 ms	748 ms	1136 ms	1030 ms
Middle Cycle VI	√	542 ms	1062 ms	1288 ms	1252 ms
Lower Cycle VI	√	752 ms	1374 ms	1556 ms	1538 ms
Top Cycle V	√	988 ms	1728 ms	1840 ms	1874 ms
Middle Cycle V	√	1802 ms	2178 ms	2264 ms	2298 ms

Table 4.2. Interpreted horizon for line CW 98-096.

Cycle	interpretation	Well B
Top Cycle VI	√	1352 ms
Middle Cycle VI	√	1696 ms
Lower Cycle VI	√	1916 ms
Top Cycle V	√	2196 ms
Middle Cycle V	√	2812 ms

Table 4.3. Interpreted horizon for line CSK2K-04A.

Cycle	Interpretation	Well A3	Well S	Well B3
Top Cycle VI	√	786 ms	804 ms	798 ms
Middle Cycle VI	√	1140 ms	1116 ms	1074 ms
Lower Cycle VI	√	1440 ms	1422 ms	1428 ms
Top Cycle V	√	1920 ms	1896 ms	1896 ms
Top Cycle V	√	2520 ms	2514 ms	2538 ms





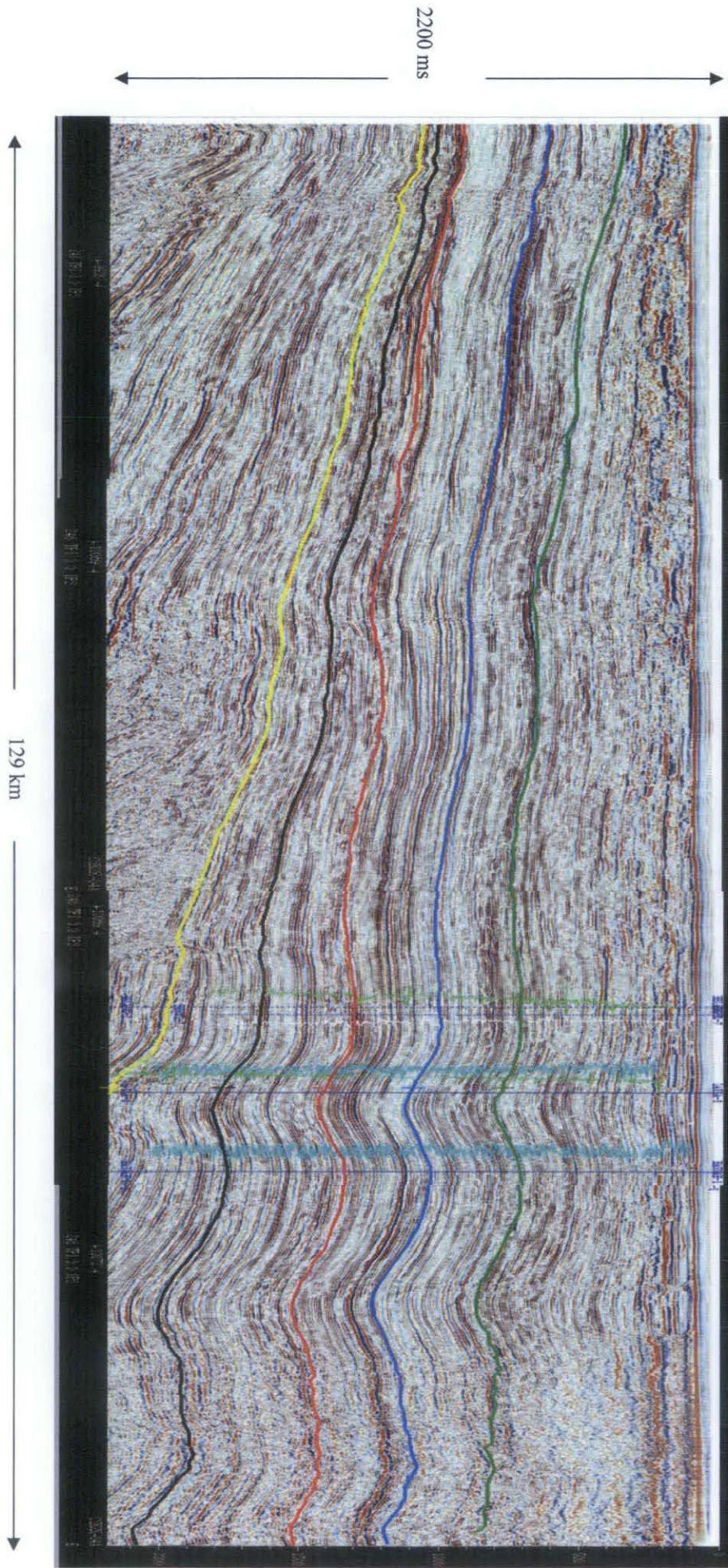


Fig. 4.2 Seismic line CSK2K-04A

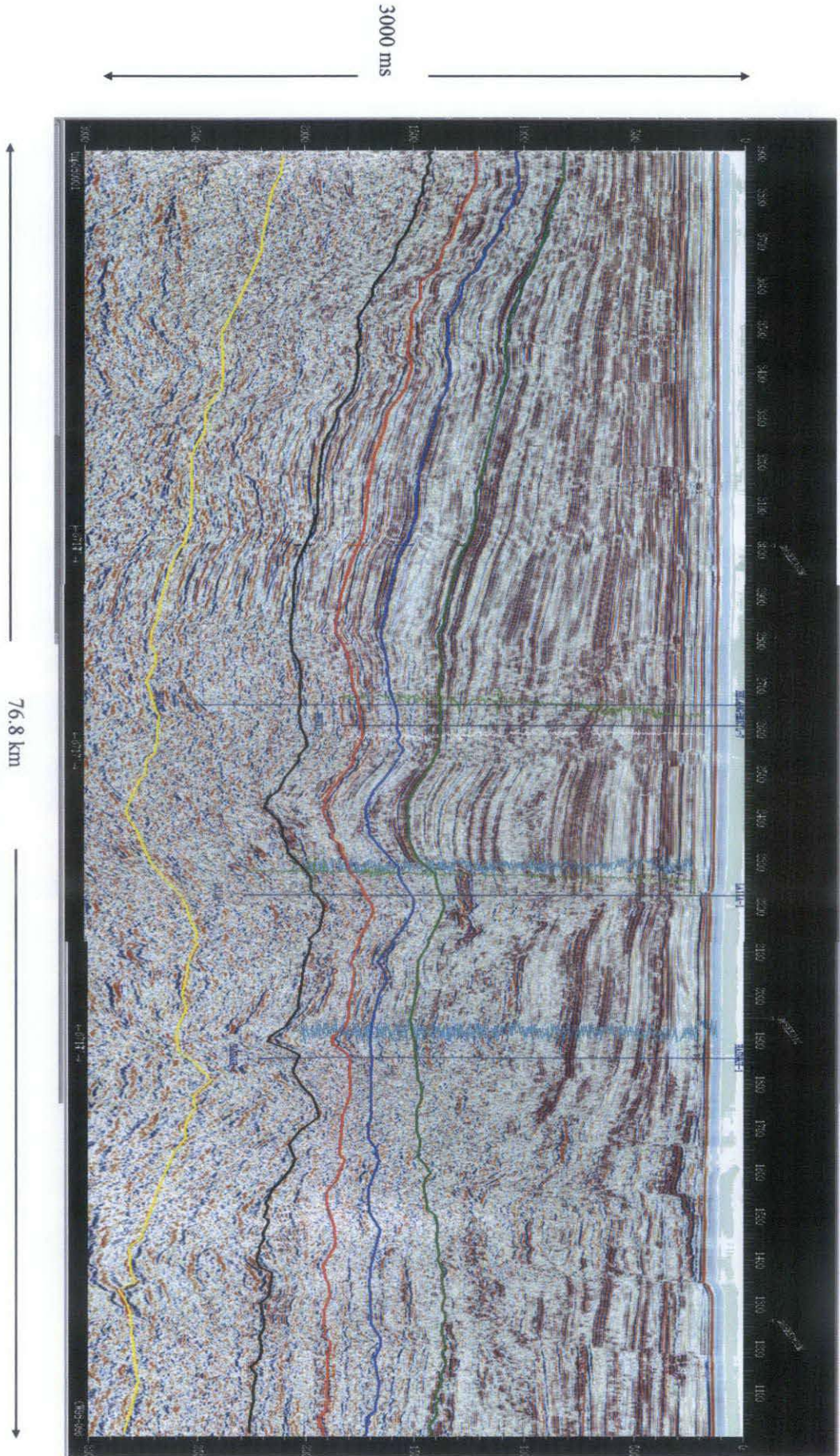


Fig. 4.3 Seismic line CW 98-096

## 4.2 1D Modeling (Genex)

In order to perform the 1D modeling, data such as temperature and vitrinite reflectance need to calibrate the heat flow. However, not all wells are well calibrated with both temperature and vitrinite reflectance. Mostly, the vitrinite reflectances are not well calibrated. This may be due to vitrinite suppression whereby the sample had been impregnated with oil, thus affecting the accuracy of the vitrinite reflectance measurements (Figure 4.5). Weathering of the sample, if the sample had been eroded and exposed, can also influence the accuracy of the measurement. The vitrinite sample that had been eroded, recycle and redeposited also influence the measurement of vitrinite reflection (Figure 4.6). Since the temperature data is more reliable (temperature from production tests), by calibrating the temperature, assumptions were made that the heat flow is acceptable. In this study, an assumption is made, that the heat flow in the past was similar to the present day. This assumption was made because the VR data is unreliable. This assumption works well in D, thus justifying the application to other wells. The present day temperatures are well calibrated all the wells (Figure 4.4, 4.6, 4.8, 4.10, 4.12, 4.14, 4.16, 4.18, and 4.22). The vitrinite reflectances of the wells that are not well calibrated due to vitrinite suppression are Well D (Figure 4.5), Well A (Figure 4.7), Well G (Figure 4.9), Well I (Figure 4.11), Well H (Figure 4.13), Well F (Figure 4.15), Well J (Figure 4.17). The vitrinite reflectance in Well C (Figure 4.19) and Well B (Figure 4.21) are eroded and redeposited. While in Well E (Figure 4.23), the vitrinite suggests the possibility of the occurrence of both vitrinite erosion and redeposition and suppression occurring simultaneously.

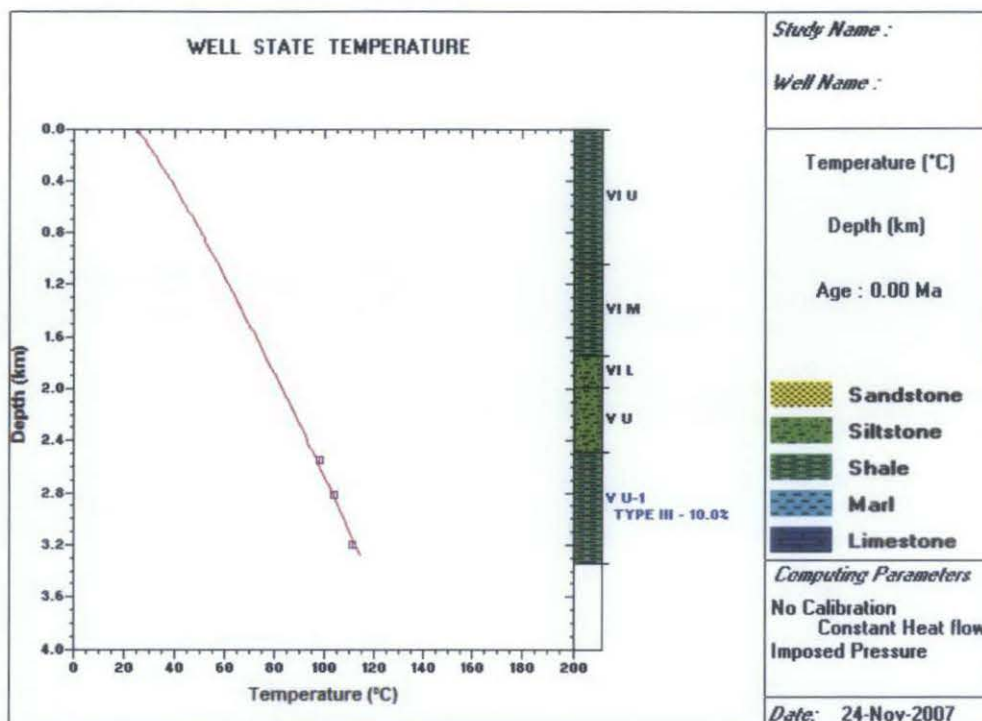


Fig. 4.4. The temperature in Well D is well calibrated with the temperature.

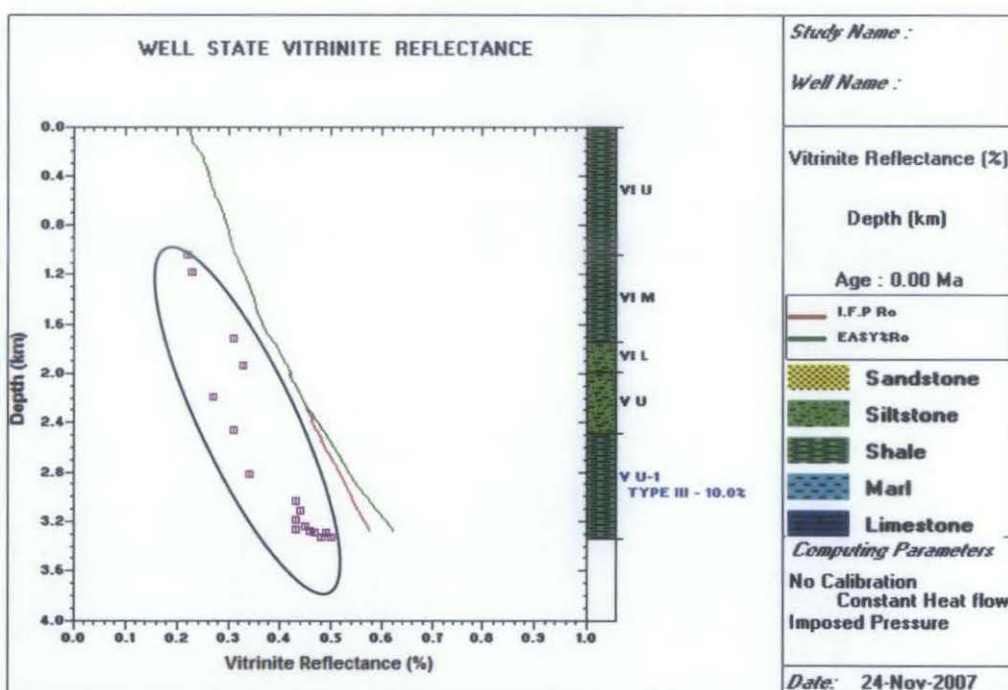


Fig. 4.5 The vitrinite reflectance is not well calibrated. The vitrinite reflectance value indicate a lower heat flow in the past, possibly due to vitrinite suppression, whereby the sample had been impregnated by oil.

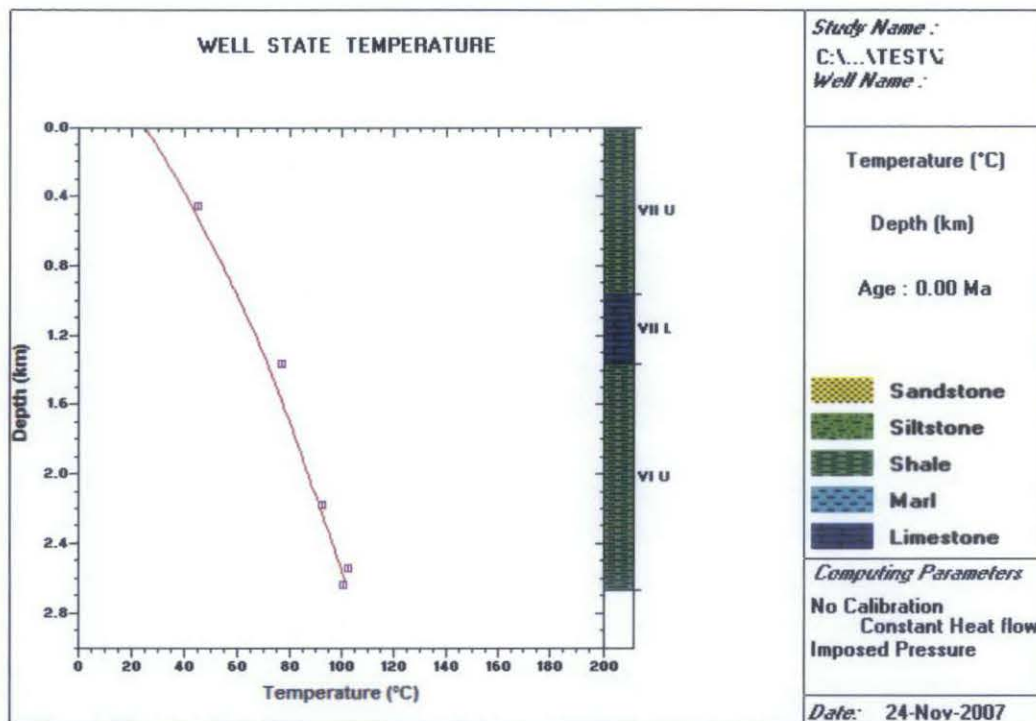


Fig.4.6. The temperature in well A is quite well calibrated

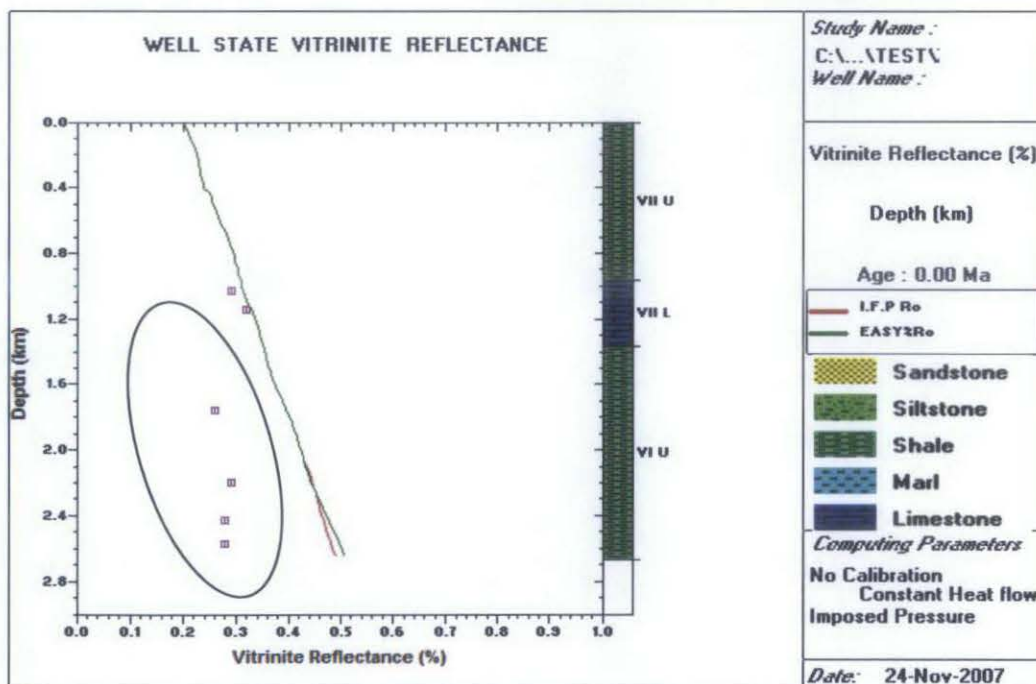


Fig. 4.7. The vitrinite reflectance in Well A is suppressed.

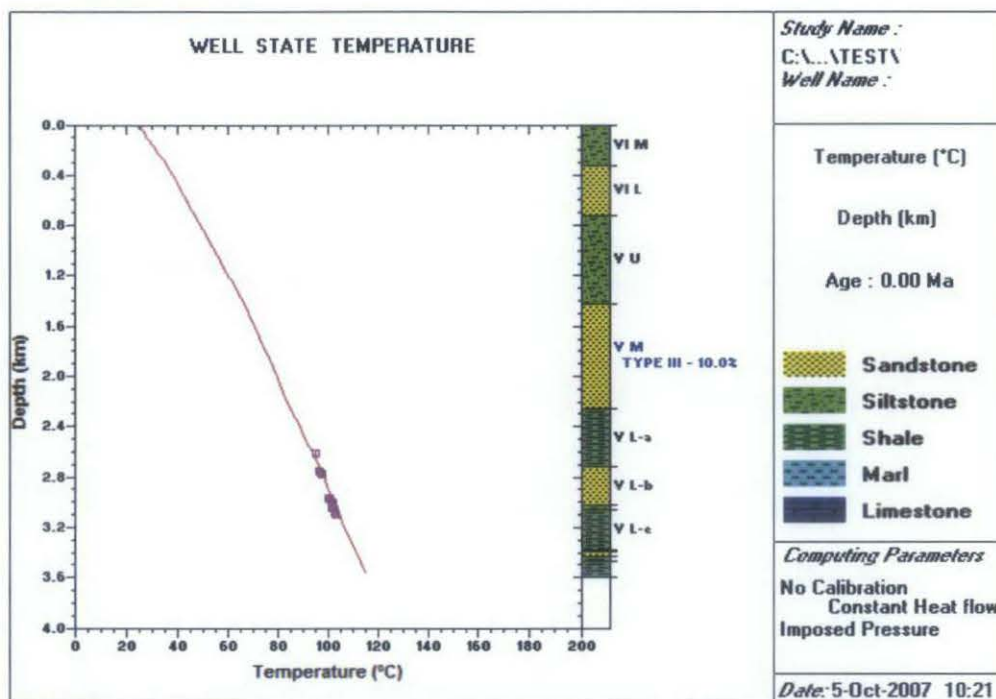


Fig. 4.8 The temperature in Well G is well calibrated.

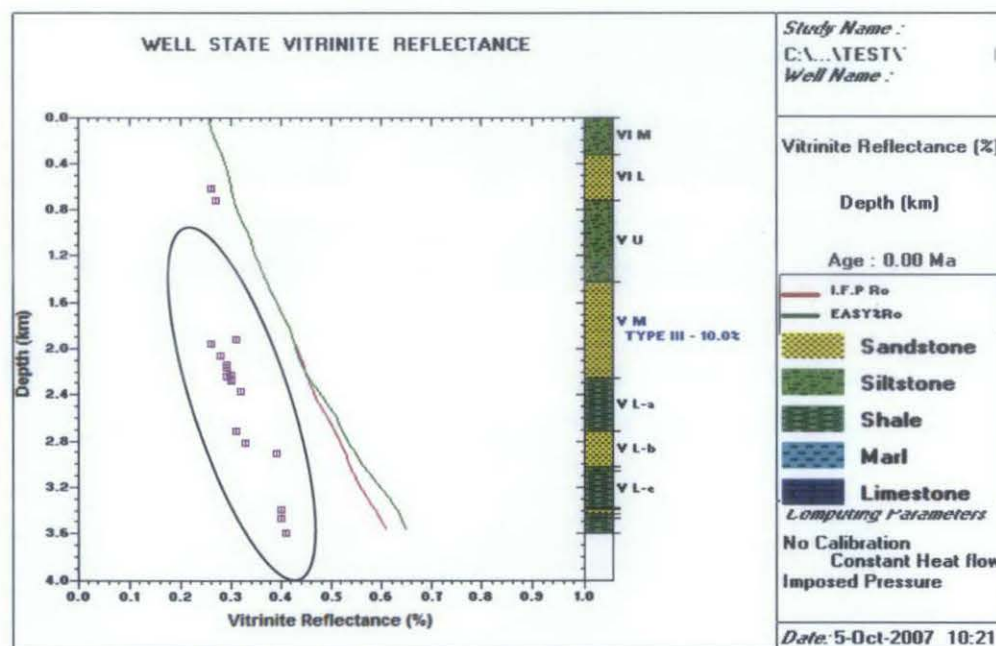


Fig. 4.9. The vitrinite reflectance in Well G is suppressed.

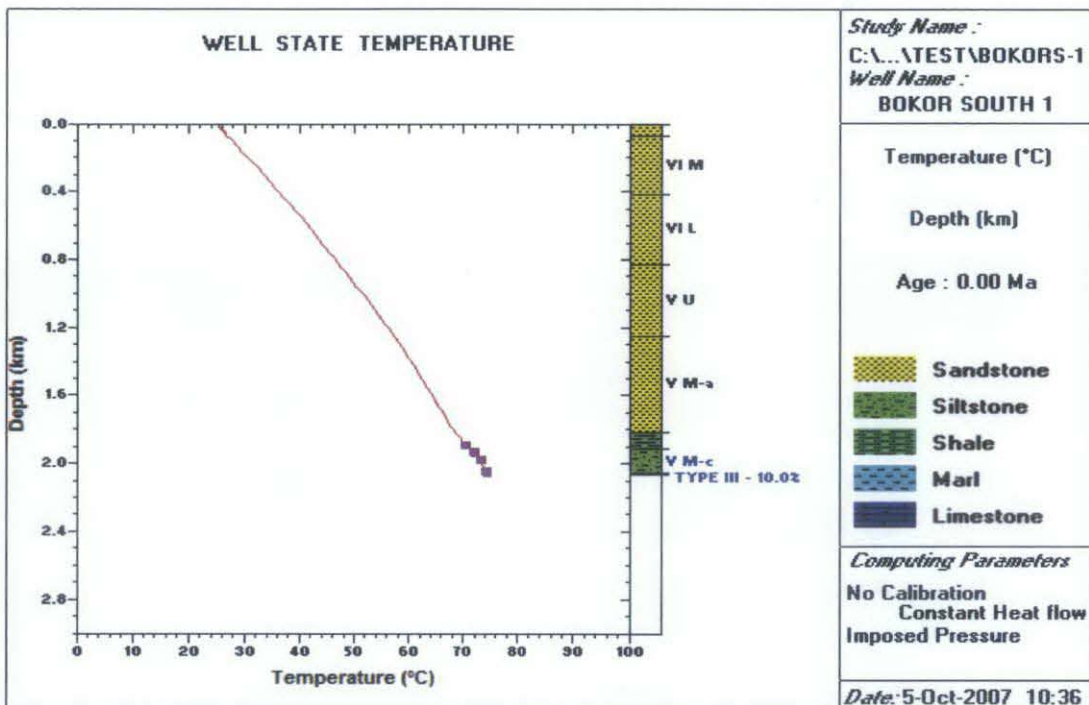


Fig. 4.10 The temperature in well I is well calibrated.

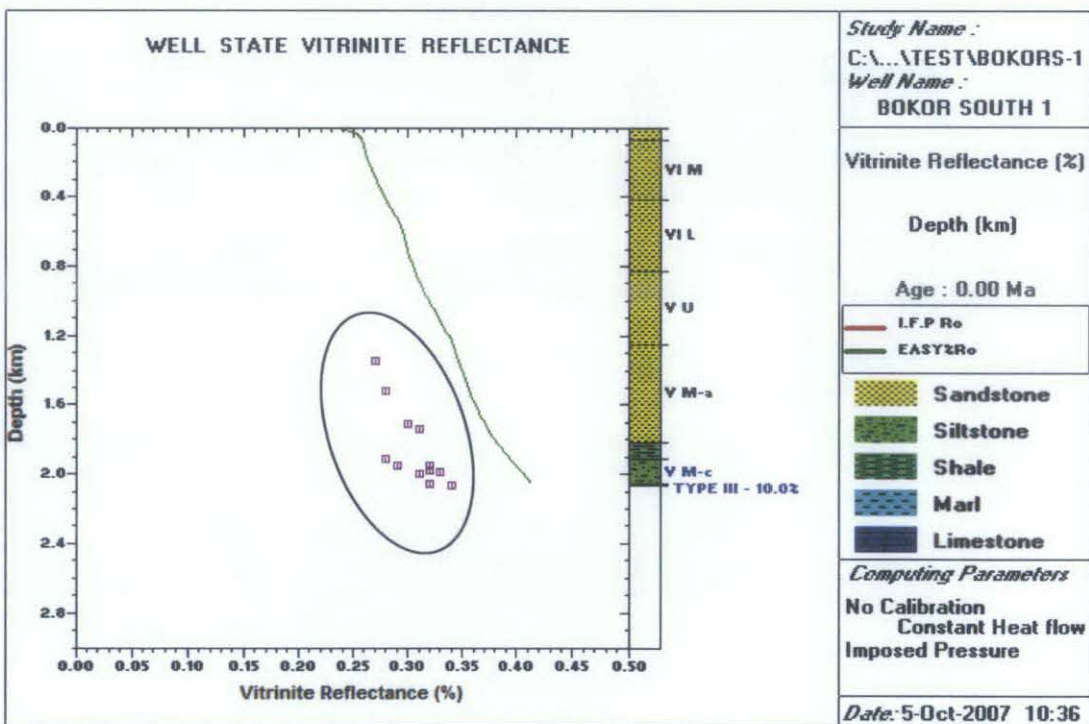


Fig. 4.11 The vitrinite reflectance in Well I is suppressed.

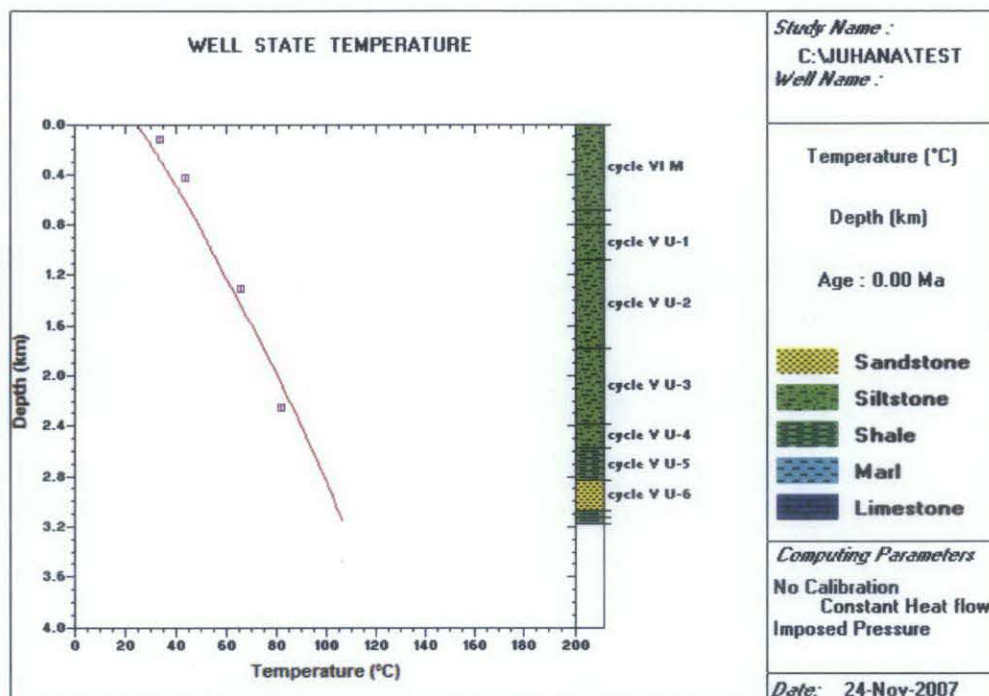


Fig.4.12. The temperature in Well H is well calibrated.

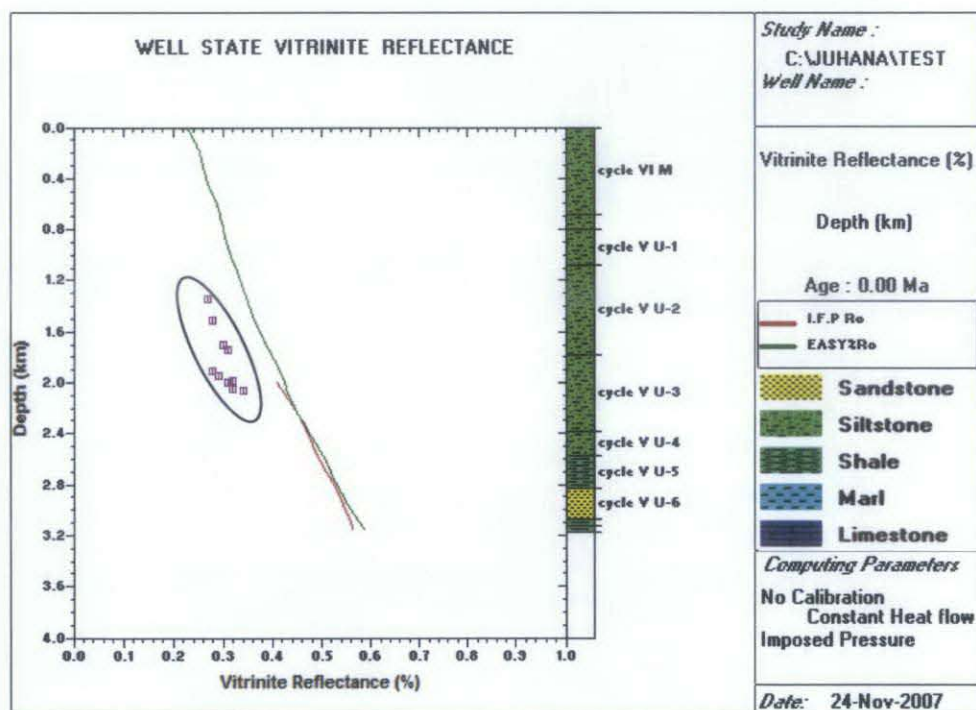


Fig.4.13. The vitrinite reflectance in Well H is suppressed.



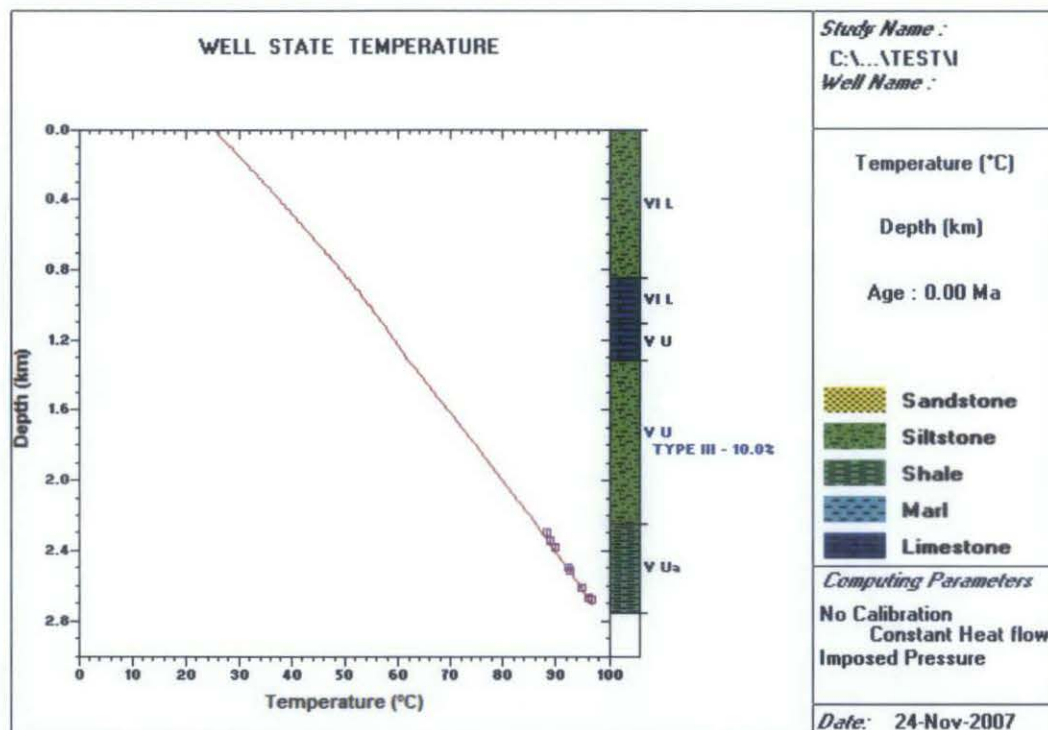


Fig 4.14. The Temperature in Well F is well calibrated.

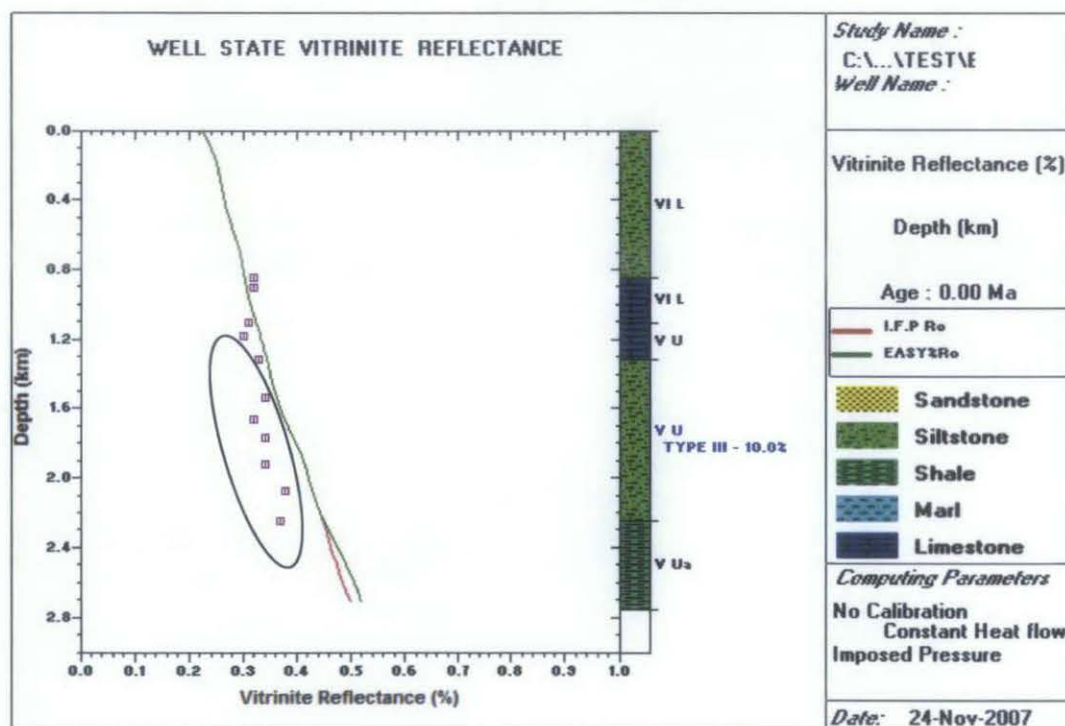


Fig. 4.15. The vitrinite reflectance in Well F is suppressed.

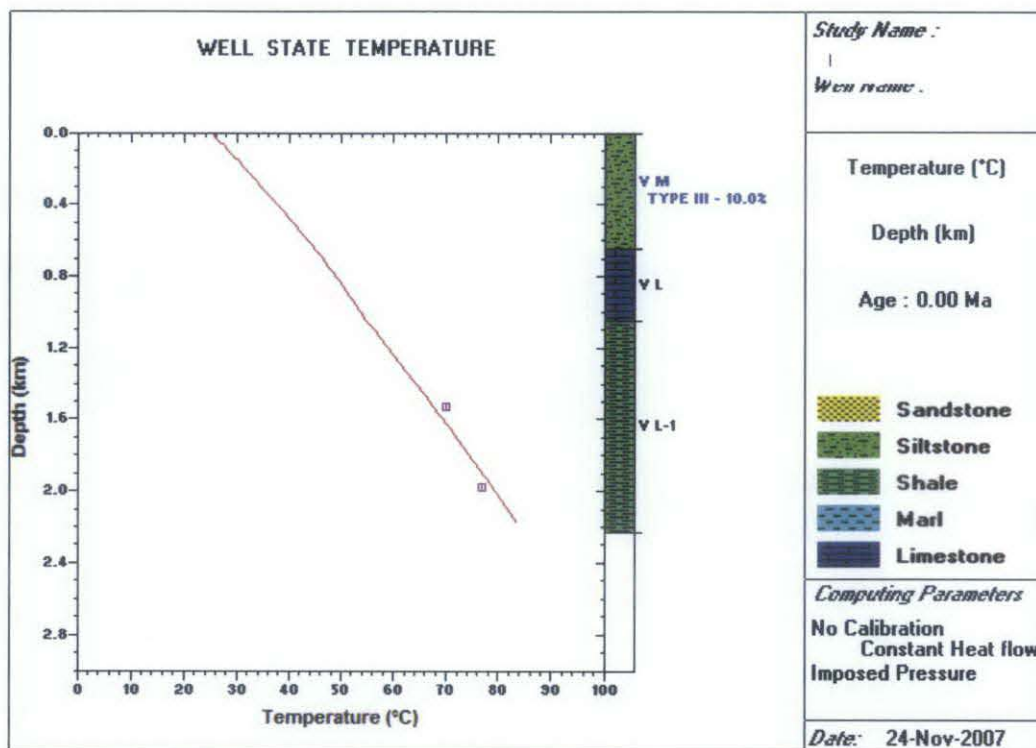


Fig. 4.16 The temperature in Well J is well calibrated.

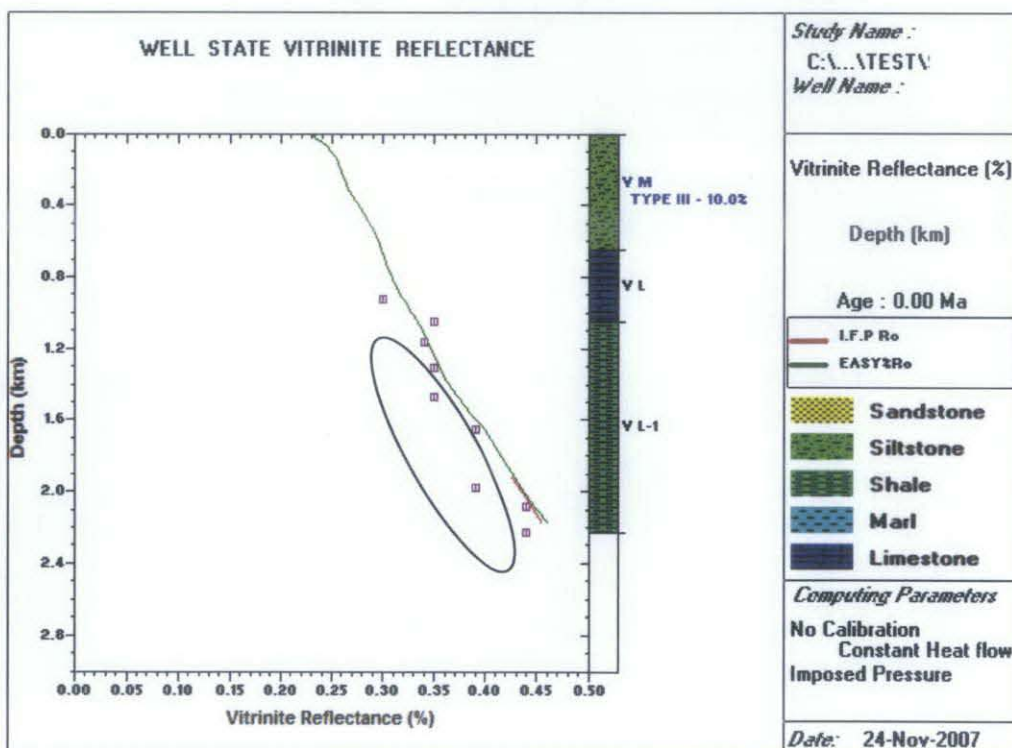


Fig. 4.17. The vitrinite reflectance in Well J is suppressed.

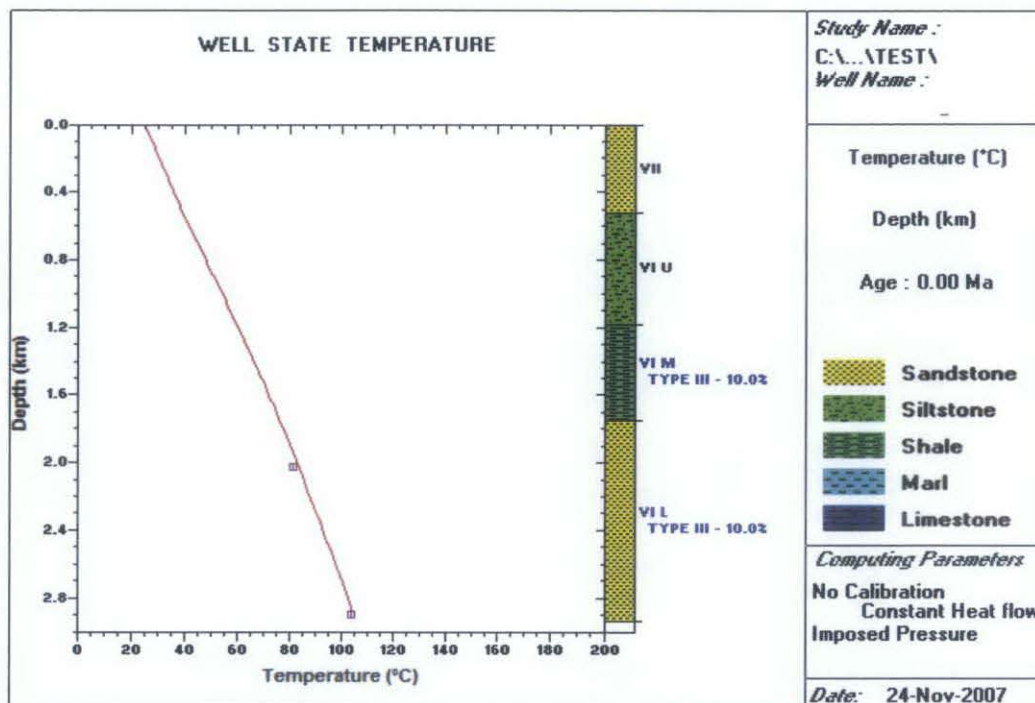


Fig.4.18. In Well C, the temperature is well calibrated.

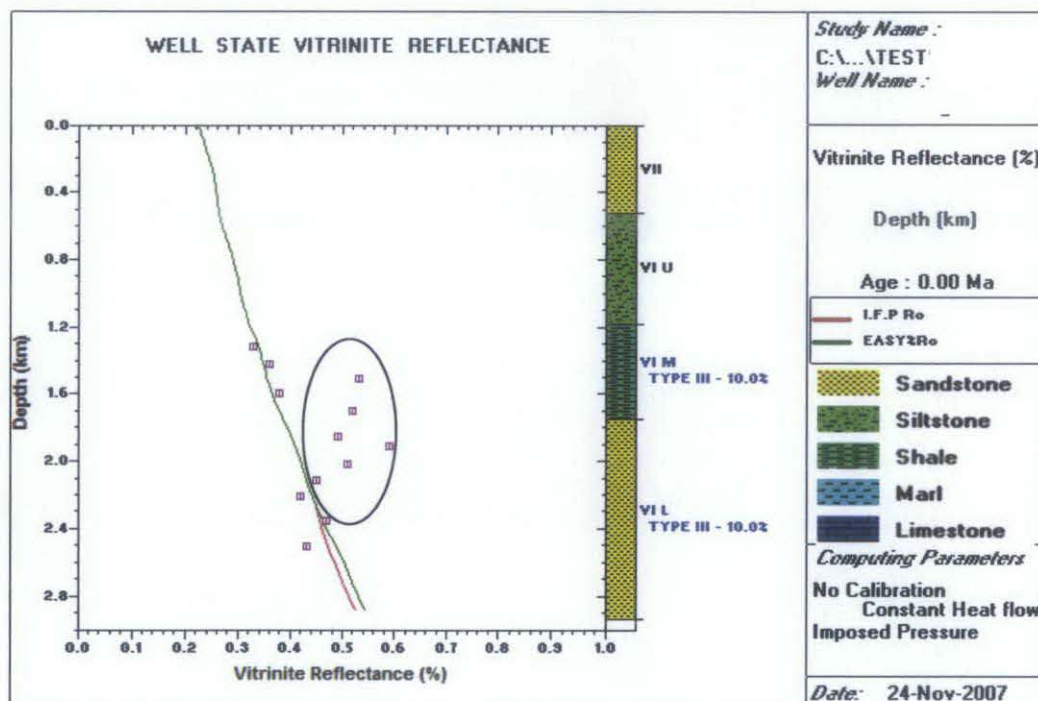


Fig. 4.19. The vitrinite reflectance is not well calibrated in this well. The vitrinite reflectance indicated that the past temperature is higher than the temperature in present day. This is possibly due to vitrinite was recycling where the sample could have been eroded from another place that had higher past temperatures where redeposited in this area.

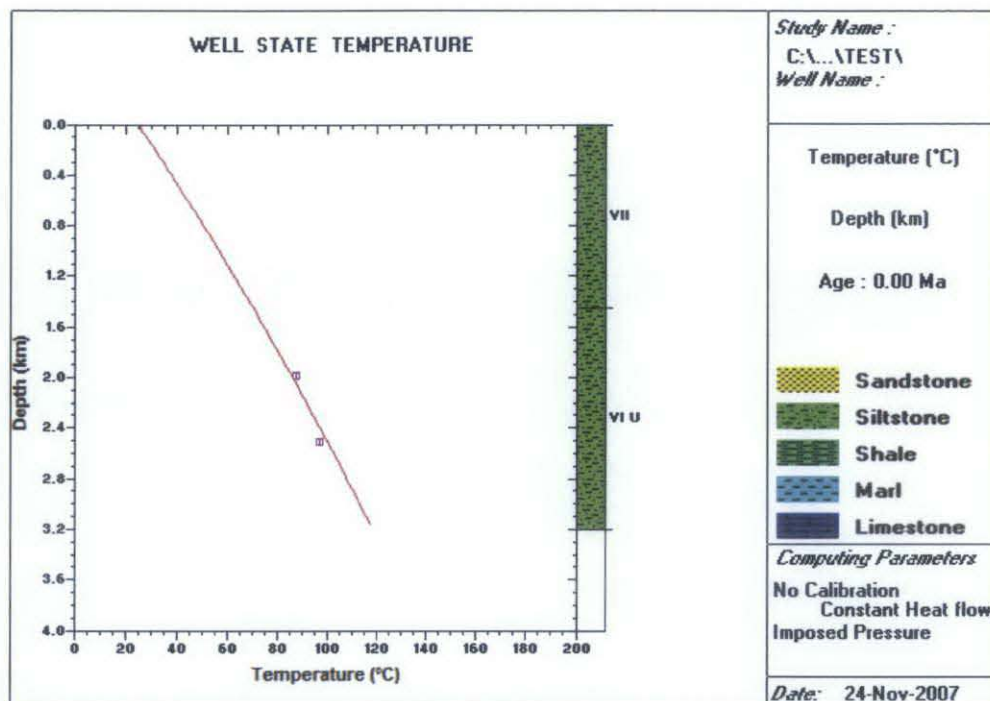


Fig. 4.20. The temperature in Well B is well calibrated.

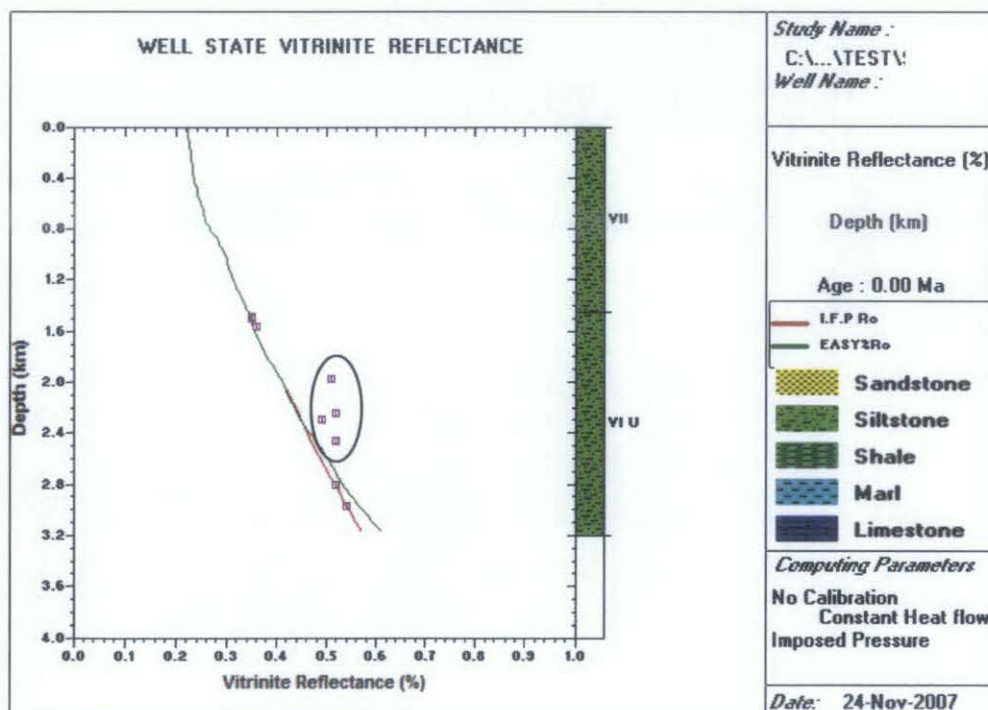


Fig 4.21. The vitrinite reflectance in Well B is eroded and recycled.

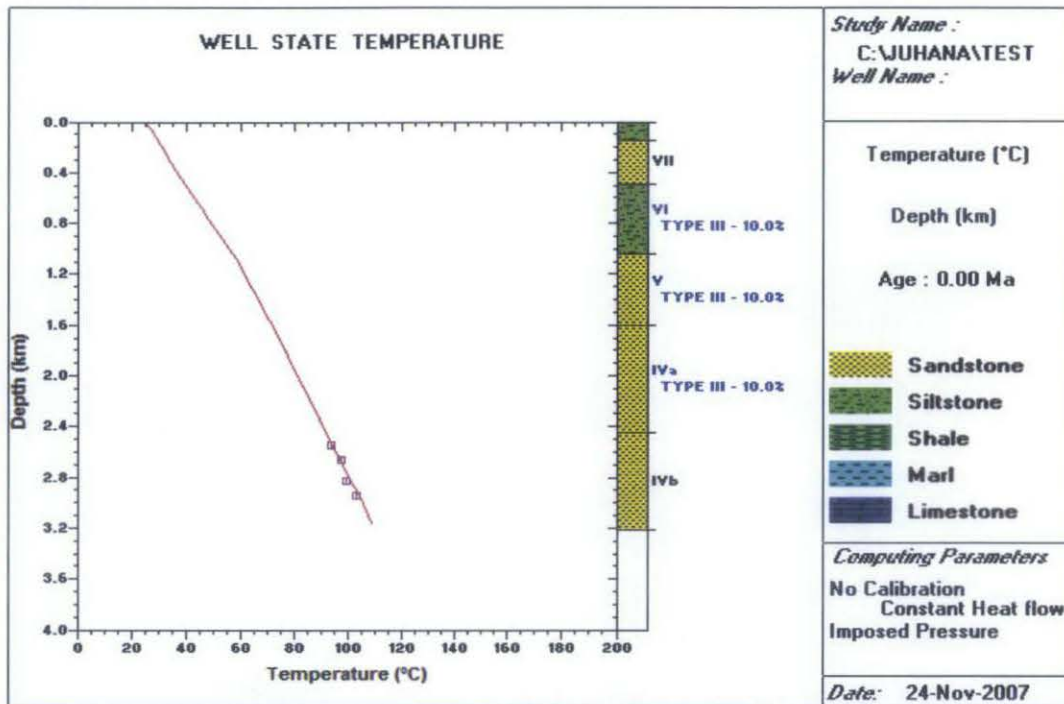


Fig.4.22. The temperature in Well E is well calibrated.

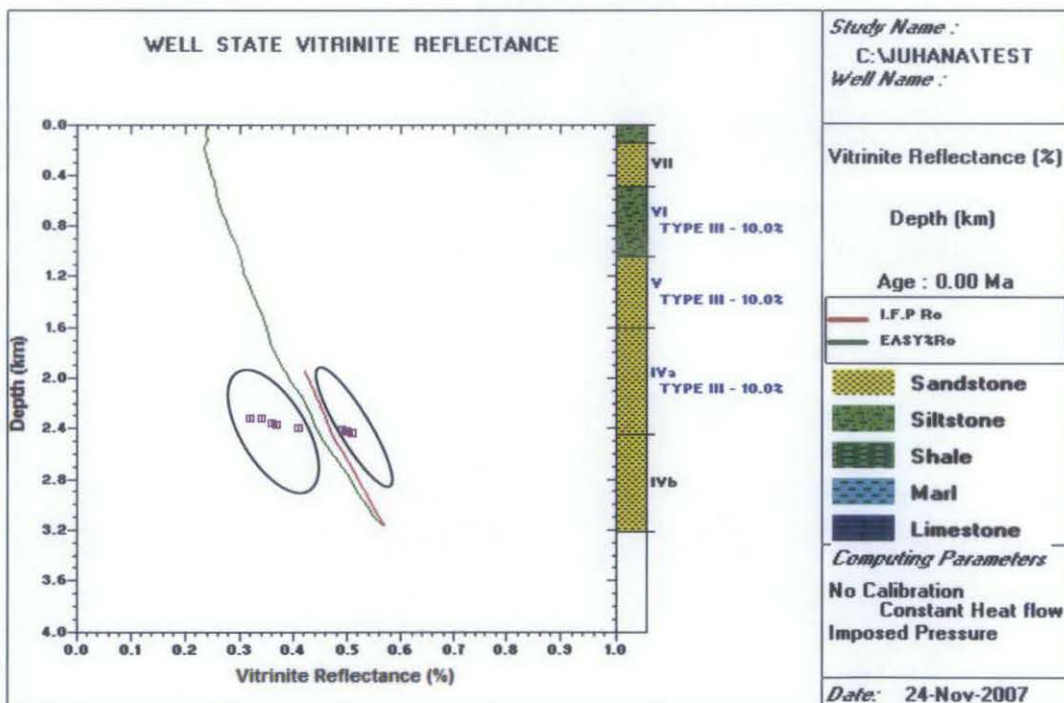


Fig. 4.23. The vitrinite reflectance in Well E indicate the presence both eroded and recycled, and suppressed vitrinite.

There are two scenarios regarding the vitrinite reflectance that does not fit with the calibrated heat flow. The first scenario is that the temperature data is correct and the vitrinite reflectance is suppressed or recycled. In the second scenario, the vitrinite reflectance is correct which shows that the temperature was very low in the past. Commonly, the scenario is more typical. This supported by study from Azlina Anuar and Peter Abolins (2005) and Zielinski et. al. (2005). Azlina Anuar & Peter Abolins (2005) also reported the heat flow values increasing seaward in the Sabah Basin, thus supporting the trend observed here. A similar trend in the offshore Brunei area, Zielinski et. al. (2005) also reported that on the Brunei continental margin. In seaward area, the mean heat flow is  $59.0 \pm 22.6$  mW/m<sup>2</sup> and in the landward area, the mean heat flow is  $83.7 \pm 66.5$  mW/m<sup>2</sup>.

Below are the wells for which 1D modeling was undertaken for heat flow determination (Table 4.4). All the wells are not well calibrated. Well A, D, F, G, H, I, J are not well calibrated due to vitrinite suppressions. While well B and Well C are not well calibrated with vitrinite reflectance may be due to the sample have been eroded and redeposited. In well E, the calibration of vitrinite reflectance is not good and it shows that the samples may have been eroded and redeposited, and/or suppressed.

Table. 4.4 Selected well for 1D modelling.

Wells	1 D model	Heat flow (mW/m <sup>2</sup> )
A	√	53
B	√	54
C	√	43
D	√	39
E	√	37
F	√	32
G	√	35
H	√	30
I	√	30
J	√	25

Abdul Jalil Muhammad & Azlina Anuar (1999) cited that the heat flow in West Baram Delta is 65 mW/m<sup>2</sup>. From this study, the heat flow from the 1D modeling ranging from 53 mW/m<sup>2</sup> to 25 mW/m<sup>2</sup>. It was observed that heat flow

increases seawards (Figure 4.24). This may be related to the low sedimentation rates in the distal area and high sedimentations rates in the proximal. In the landward area, the sedimentations rates are high, while in the seaward areas the sedimentation rates are relatively lower. The high sedimentation rates create a condition called a transient state (unsteady state). The thick sediment in the landward area need higher value of heat flow to heat up the cold sediments thus the temperature is reduced quickly, therefore heat flows are low. Since the burial is fast in high sedimentations rates, water along with the heat can escape quickly from pore pressure, resulting low heat flows.

In the seaward area, the heat flow is high due to the relatively lower sedimentation rates, creating a steady state condition. In this steady state regime, the temperature is evenly distributed from the heat flow. So, this is why the heat flow is high in areas with low sedimentation rates. The heat flow mentions here are basement heat flow.

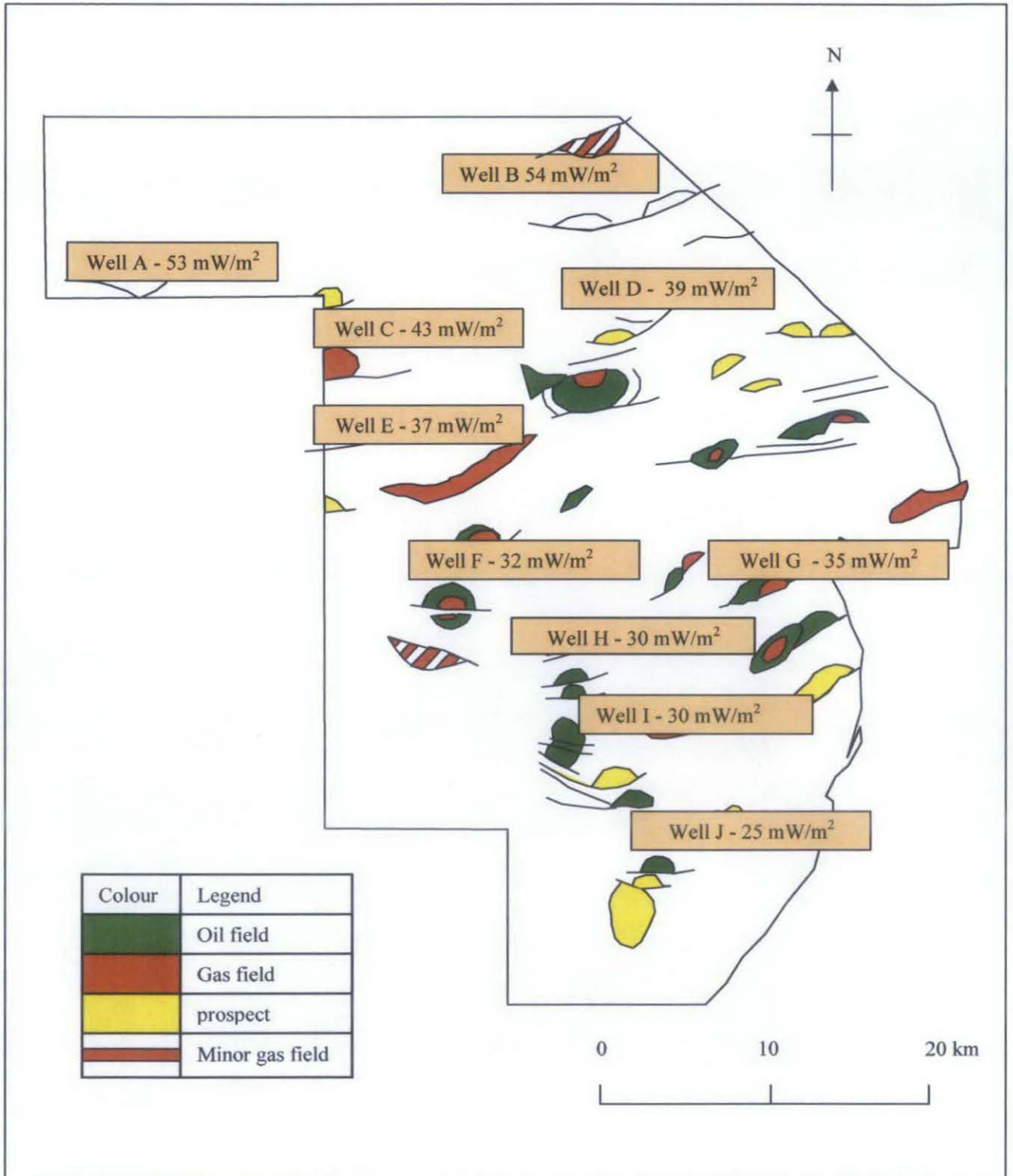


Fig. 4.24. Modeled heat flow distribution in the Baram Delta.



### 4.3 Pore Pressure Estimation

Figure 4.25 shows the selected wells for pore pressure estimation using Drillworks predict. The selected wells are Well H and Well O.

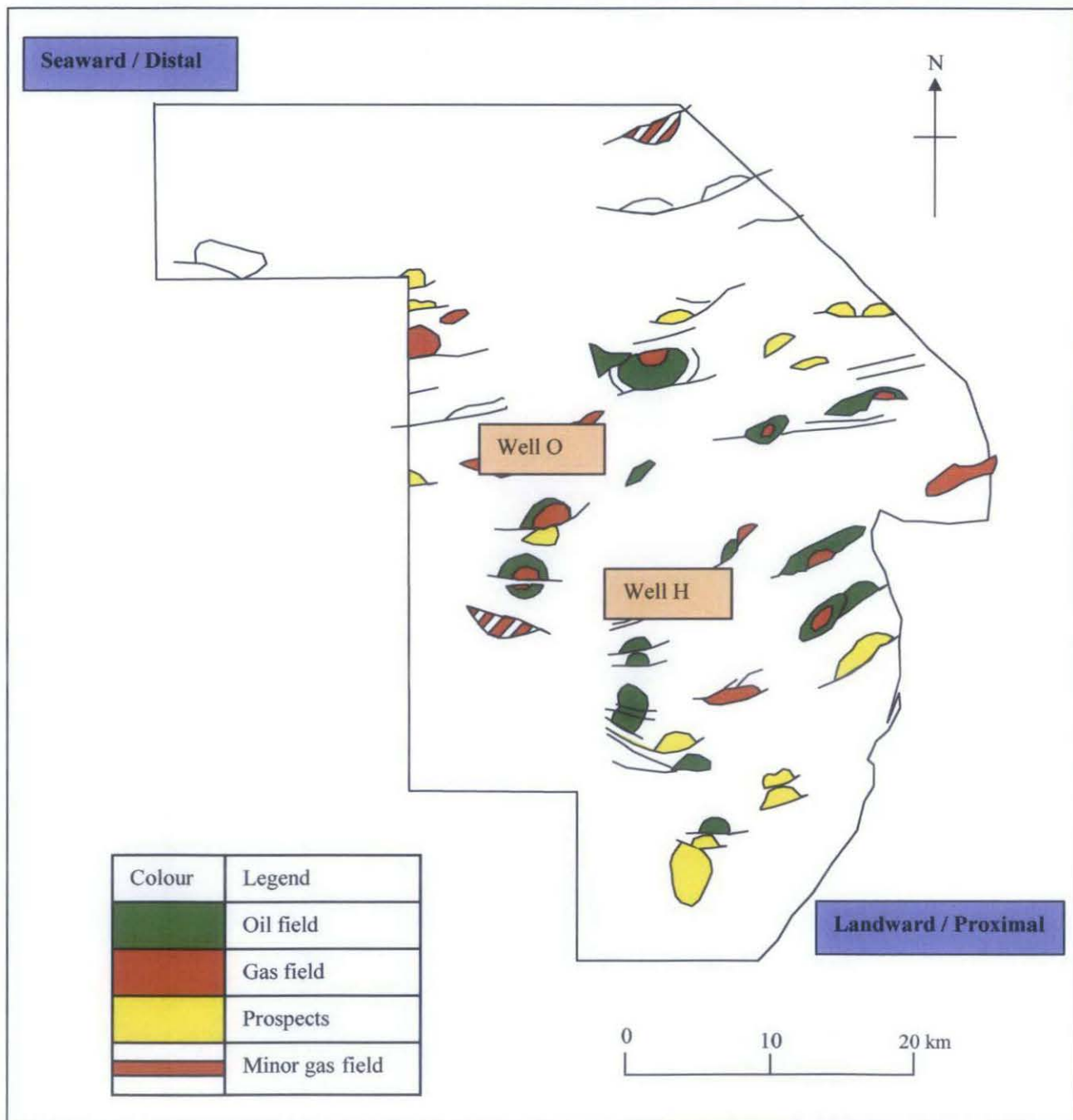


Fig. 4.25. Well H and Well O for pore pressure estimation using Drillworks Predict.

Pore pressure estimation is done by applying the Drillworks Predict software in deriving normal compaction trend. The sonic Eaton method is preferred due to its appropriate calculation. Miller methods have been applied in this study, but shows no overpressure occurs. Since the well data shows that the overpressures occur, another method was selected. By using Eaton method, the overpressure can be calculated. Thus sonic Eaton method is preferred. From this analysis, we can calculate the normal compaction trend and the pore pressure. Below are the calculated normal compaction trend calculated (Figure 4.26).

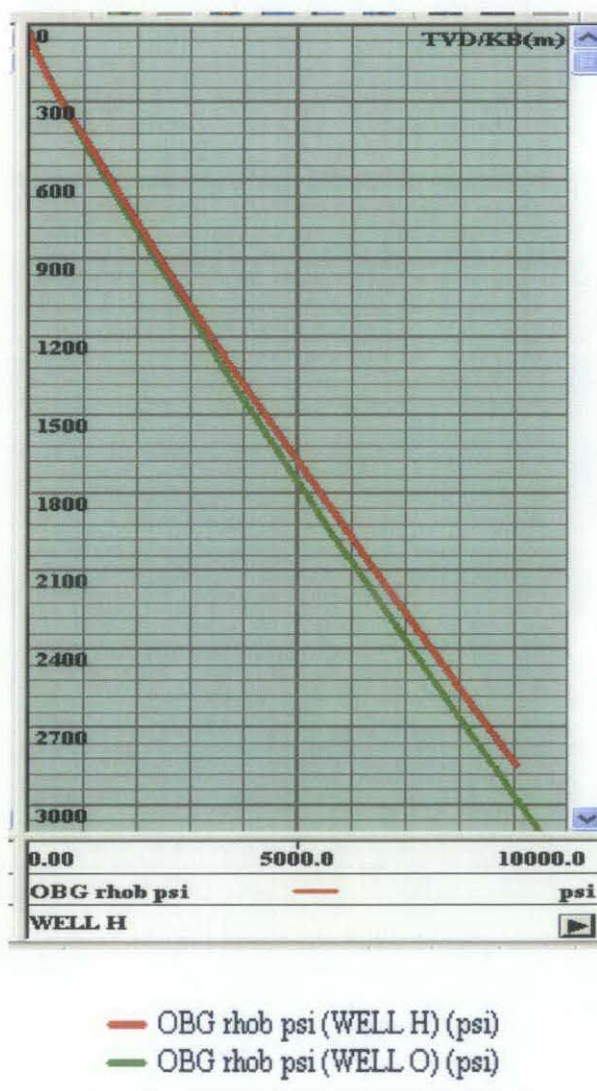
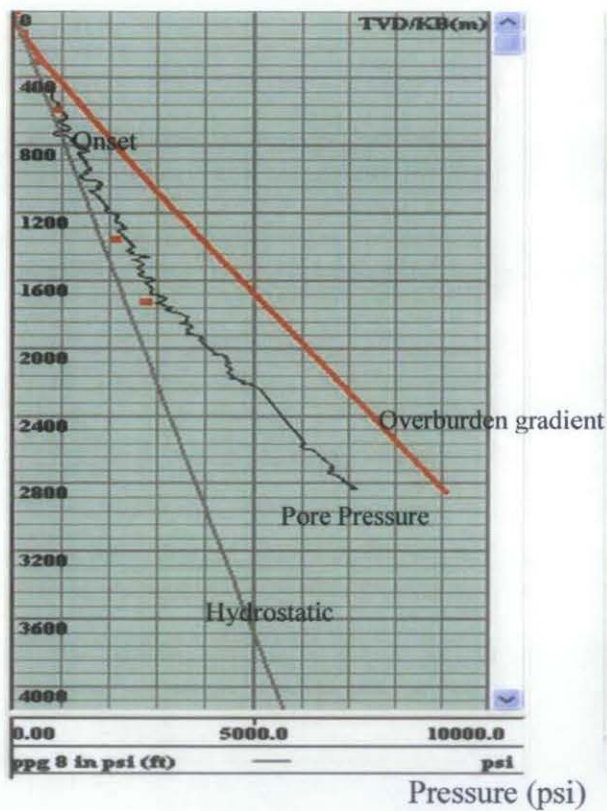


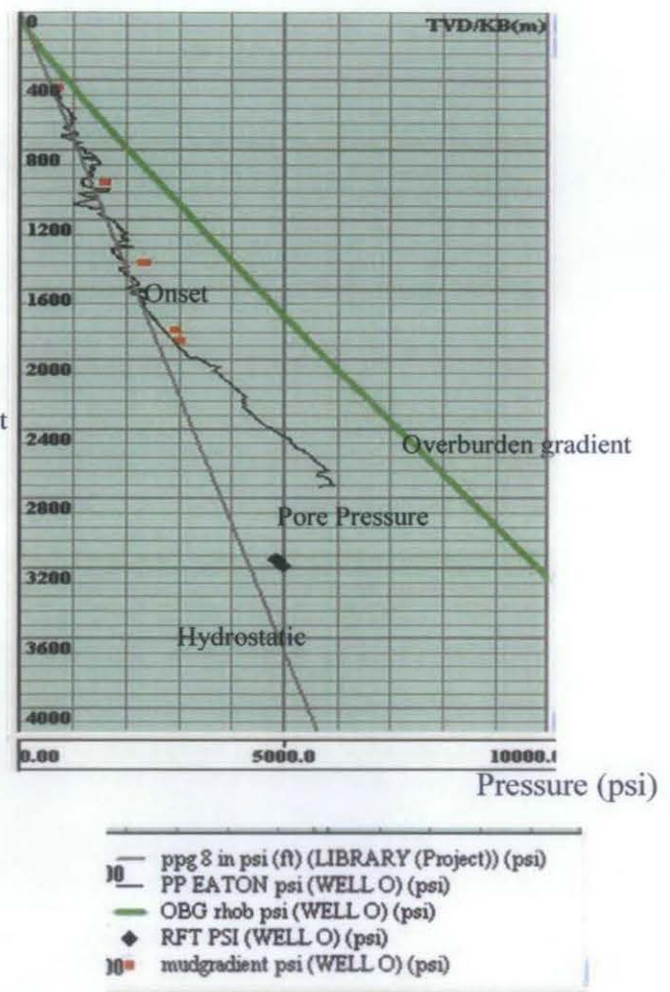
Fig. 4.26. The overburden gradient trend for Well H and Well O.

Depth (m)



Well H

Depth (m)



Well O

Fig. 4.27. The pore pressure estimation for Well H and Well O

Figure 4.27 shows the pore pressure estimation using the sonic Eaton method. Overpressure was indicated in both wells and in hydrostatic pressure. The overpressure of both well is due to the uplift and erosion of the delta hinterland (Tingay et. al., 2002).

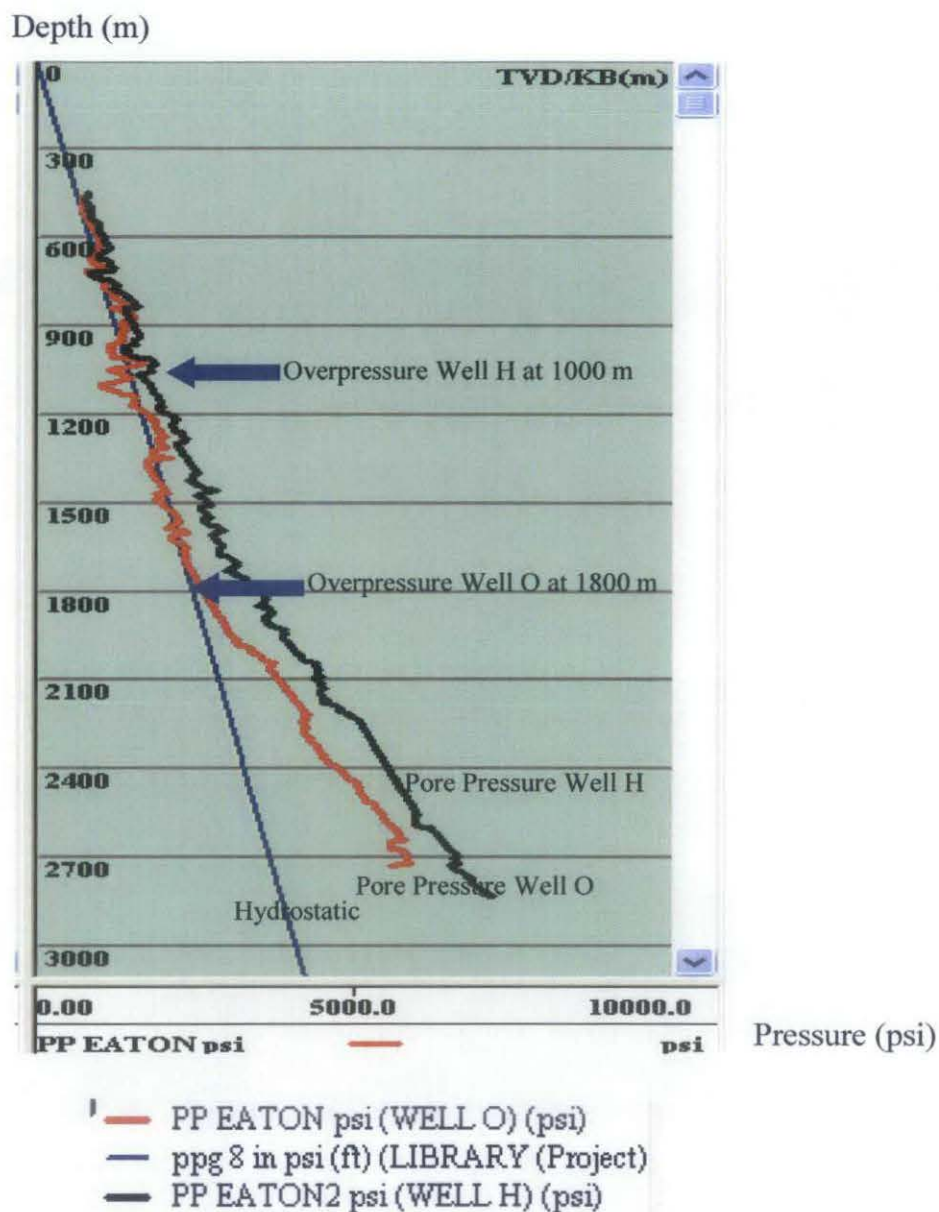


Fig. 4.28 Comparison of pore pressure between Well O and Well H.

Figure 4.28 shows the comparison of pore pressure between Well H and Well O. The top of overpressure in Well H is shallower (1000 m) than the top of overpressure in Well O (1800 m). In the proximal area, the sedimentation rate is high and burial was rapid. In the proximal area where Well H is located, the fluid in the pore cannot escape due to the rapid burial and high sedimentation rates (as high as 1550 m/Ma prevailed between 10 Ma and the present day), thus creating overpressure at a shallower depth. While overpressure in Well O is at deeper depth due to the relatively lower sedimentation rates (as high as 1300 m/Ma prevailed between 10 Ma and the present day) than in Well H, the water can escape slowly and creating a

deeper depth of disequilibrium compaction. Sedimentation rates as high as 950 m/Ma that prevailed between 10 Ma and the present day seem to preclude the development of coal rich layers in the delta (Noor Azmi Ibrahim, 1994).

#### 4.4 Depth Conversion (Easydepth)

Figure 4.29 shows the time seismic section that was imported into EasyDepth. The horizons in this time seismic section were already edited.

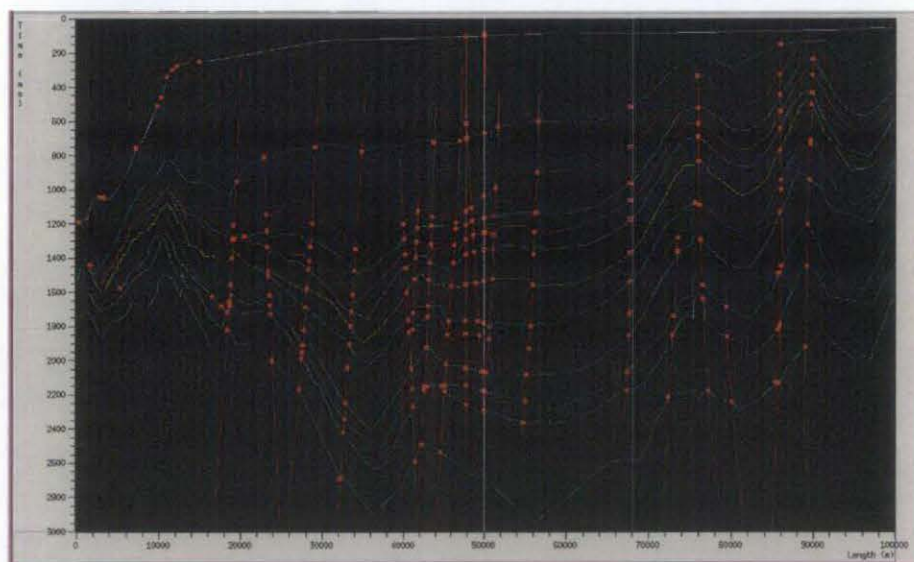


Fig. 4.29. Interpreted horizons in time.

Figure 4.30 shows the interpreted horizons in time. The velocity each layers were assigned with velocity for depth conversions and edited locally (by patches).

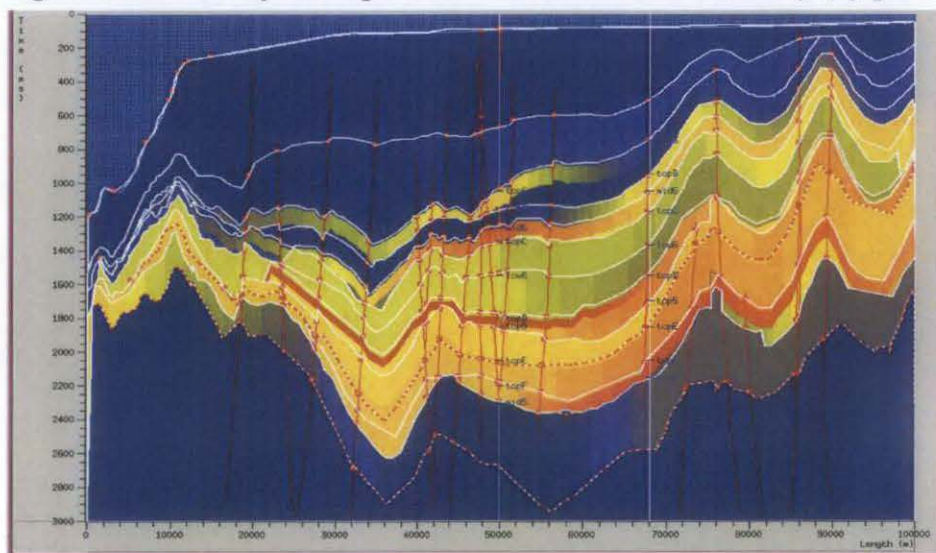


Fig. 4.30 Velocity model after edited by layers and by patches.

After the definition of the velocity for each layer, then the time seismic section is converted into depth seismic section (Figure 4.31).

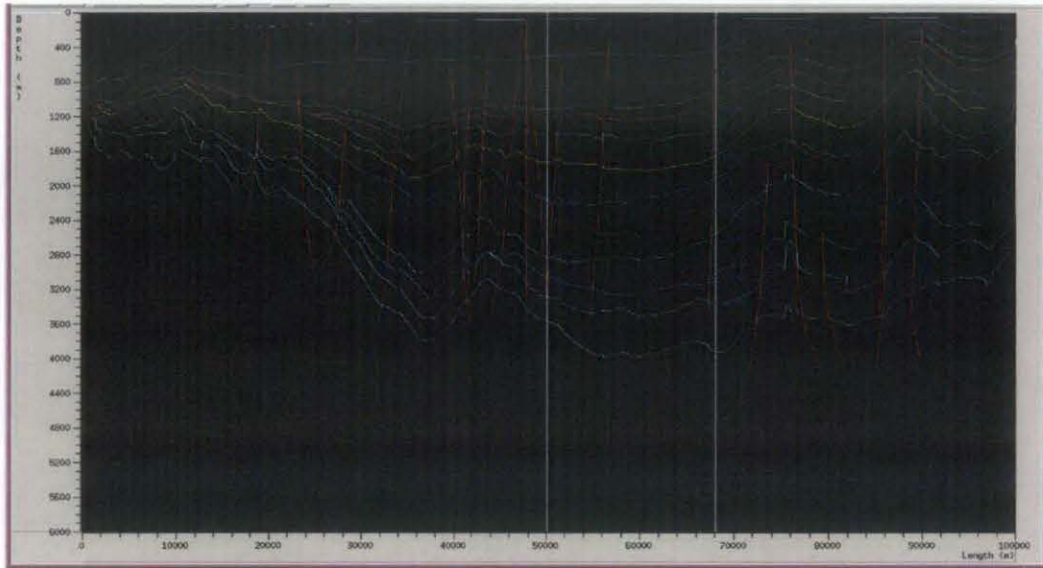


Fig. 4.31 . Depth section – converted from seismic time section.

#### 4.5 2 D Basin Modelling (Temis 2D) – Overpressure Origins

2 cases have been look into in 2D basin modelling. In the first model, the sole mechanism overpressure is the disequilibrium compaction. For the second case the model will include other possible overpressure mechanism, such as the hydrocarbon generation. Below is the lithology model in Temis 2D (Figure 4.32) and the petrophysical data of the lithology (Figure 4.33).

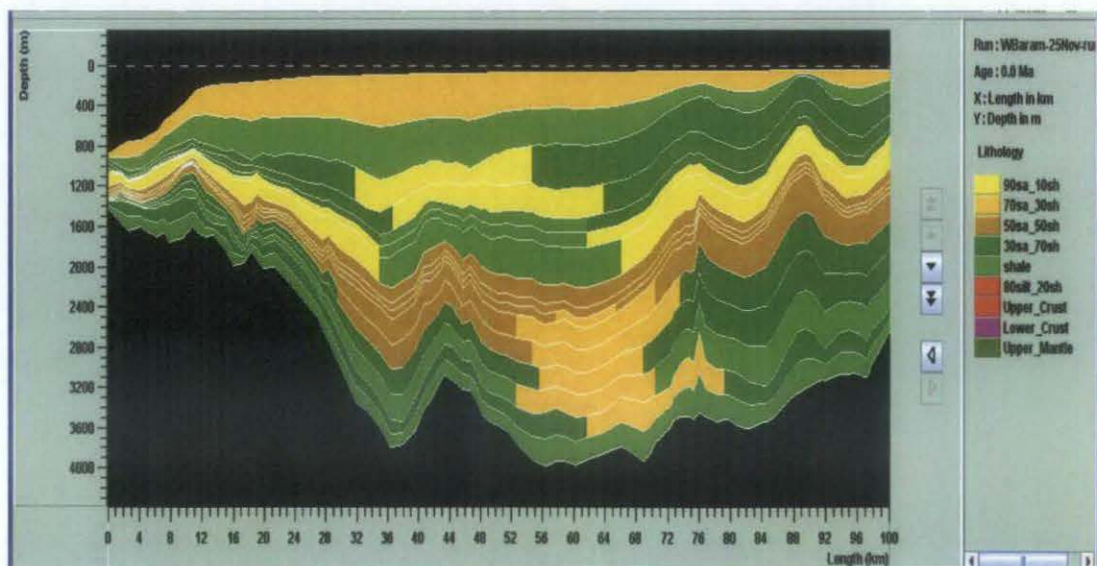


Fig. 4.32 The lithology model for disequilibrium compaction.

	Lithology Name	Color	Comment	Solid Density kg/m <sup>3</sup>	Thermal Conductivity W/mC	Specific Surface m <sup>2</sup> /m <sup>3</sup>	Mass Heat Capacity J/kg/C	Radiogenic Heat Prod. W/m <sup>3</sup>
1	90sa_10sh		subarkosic sandstone (sand 90% shale 10%)	2670.0	5.67	200000.0	710.0	6.5E-7
2	70sa_30sh		subarkosic sandstone (sand 70 % shale 30%)	2665.0	4.56	2000000.0	740.0	9.5E-7
3	50sa_50sh		subarkosic sandstone (sand 50 % shale 50%)	2660.0	3.87	5000000.0	765.0	1.25E-6
4	30sa_70sh		subarkosic sandstone (sand 10-50 % shale 50-90%)	2650.0	2.95	2.0E7	790.0	1.55E-6
5	shale		shale (90% shale 10% sand)	2645.0	2.37	1.0E8	815.0	1.85E-6
6	marl		marl	2675.0	2.76	2.5E7	810.0	1.3E-6
7	mud supported carbonate		wackestone-mudstone without early diagenesis	2710.0	3.57	1300000.0	795.0	6.2E-7
8	carbonate 100% calcite		grainstone with early diagenesis (100% calcite)	2710.0	3.57	80000.0	795.0	6.2E-7
9	carbonate 100% dolomite		grainstone with early diagenesis (100% dolomite)	2870.0	5.5	120000.0	930.0	3.6E-7
10	chalk		chalk	2710.0	3.57	2000000.0	795.0	0.0
11	salt		salt	2160.0	6.1	1.0E8	850.0	1.0E-8
12	70sh_30lst		70 shale 30lst	2750.0	2.5	1.0E7	1000.0	0.0
13	80silt_20sh		80 silt 20 shale	2750.0	2.5	1.0E7	1000.0	0.0
14	80silt_20sa		80 silt 20sa	2750.0	2.5	1.0E7	1000.0	0.0
15	50sa_50sh		50 sand 50 shale	2750.0	2.5	1.0E7	1000.0	0.0
16	80sa_20silt		80 sand 20 silt	2750.0	2.5	1.0E7	1000.0	0.0
17	water		Comment New Lithology	2750.0	2.5	1.0E7	1000.0	0.0
18	basement		Comment New Lithology	2750.0	2.5	1.0E7	1000.0	0.0

Fig. 4.33 Petrophysical data of the the lithology models.

#### 4.5.1 Disequilibrium Compaction Model

To reconstruct the pressure modeling, the model must be calibrated with the observed pressure, temperature and vitrinite reflectance dataset. Figure 4.34, the temperature in Well E is calibrated. The temperature data is from the Repeat Formation Test (RFT). From 1D Modelling (Genex) the heat flow varies from  $53\text{mW/m}^2$  to  $25\text{mW/m}^2$ . Heat flows ranging from  $53\text{mW/m}^2$  to  $35\text{mW/m}^2$  was used as an input for the heat flow in Temis 2D since the cross section for this modelling lies on this range. As the result, the temperature is well calibrated by using the heat flow modelling from 1D Genex.

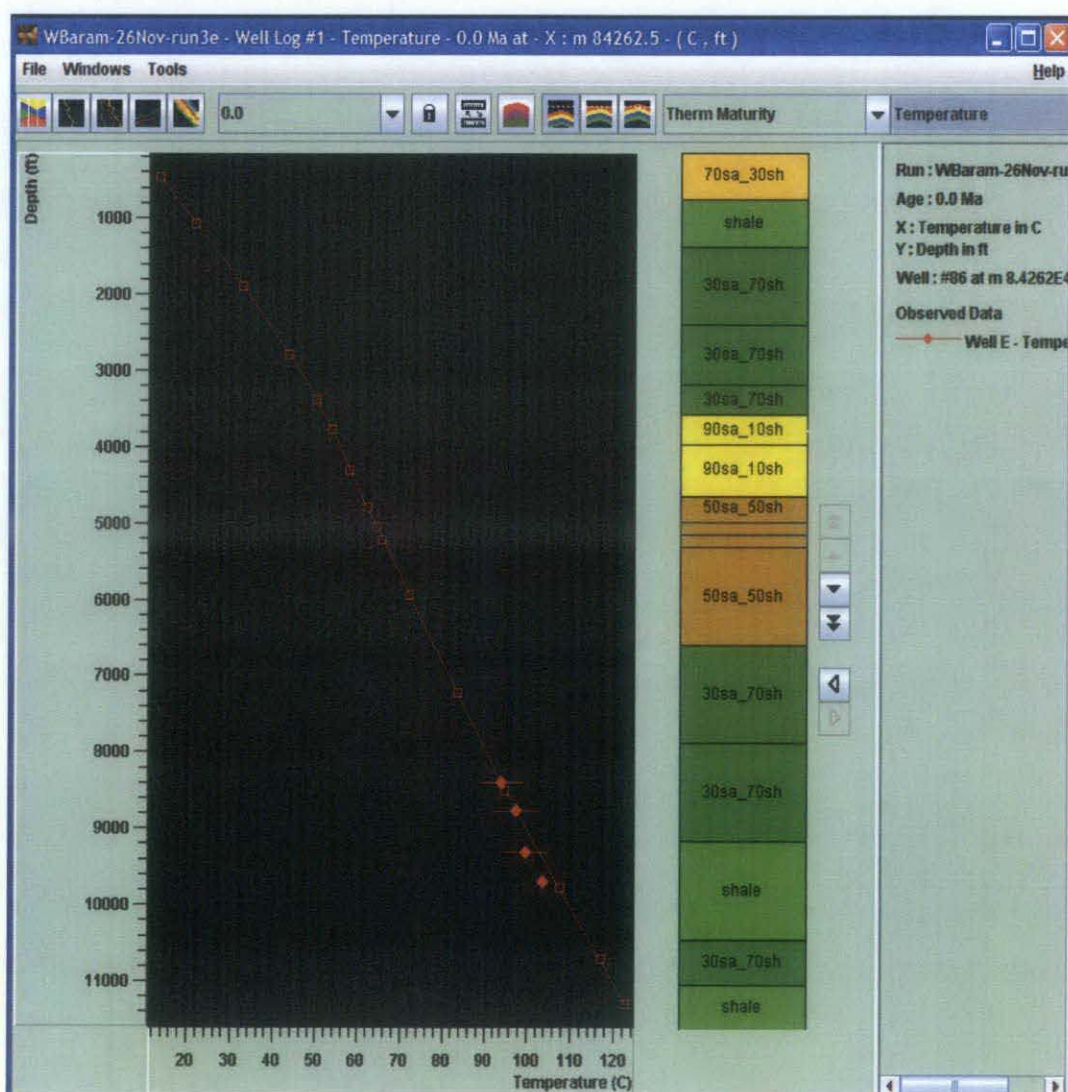


Fig. 4.34 Calibration for temperature in Well E – disequilibrium compaction.



Figure 4.35 shows the pressure calibration in Well H for disequilibrium compaction. To get a good calibration for the pressure, the permeability of the seal can be varied. The permeability can be decreased to create overpressure conditions to match the calibration data. Fluid retention leading to overpressure is largely controlled by the low permeability non reservoir rocks such as shales, evaporites and cemented carbonates (Swarbrick & Osborne, 1998).

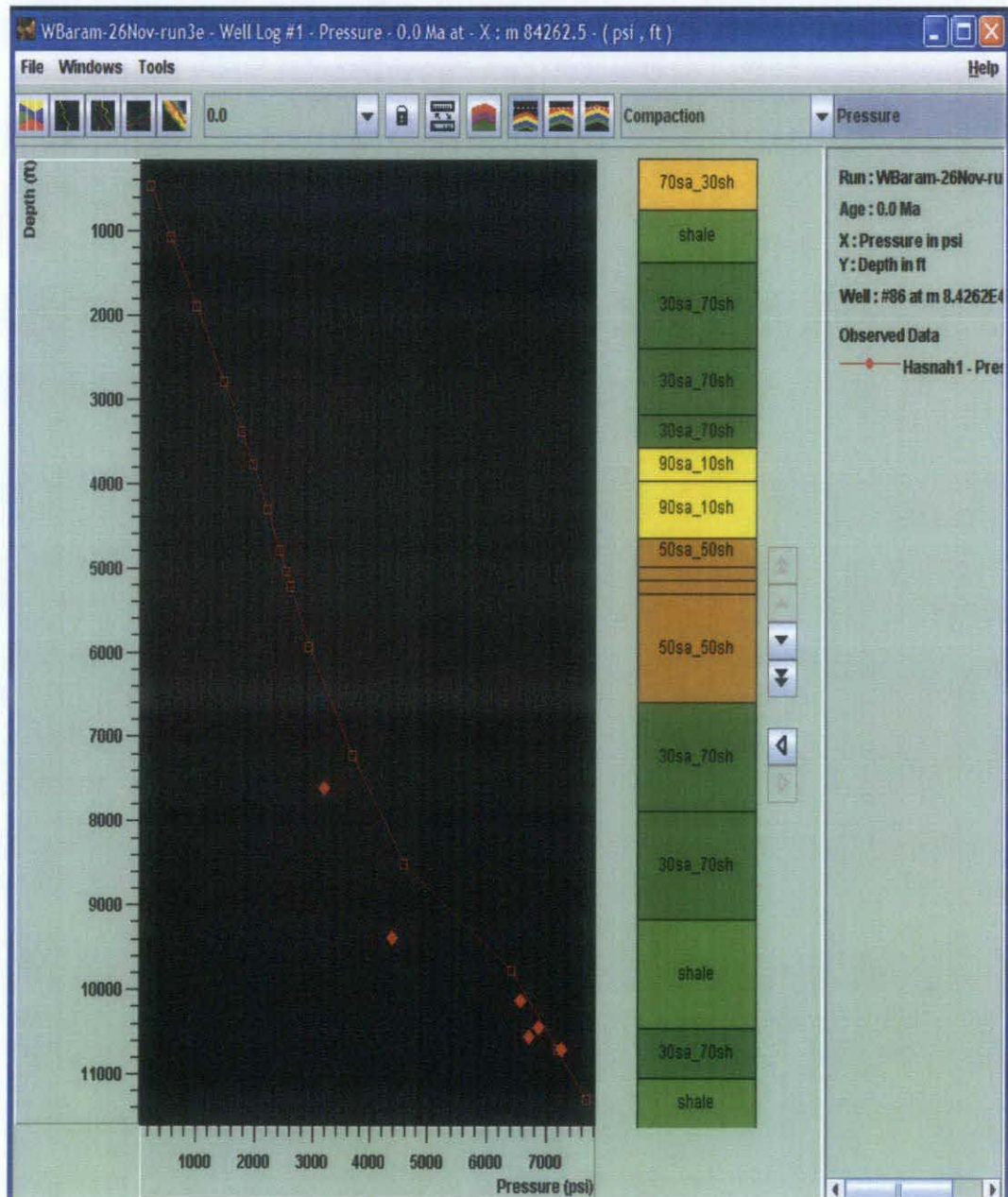


Fig. 4.35. The calibration of pressure in Well H.

Figure 4.36 shows the calibration with the vitrinite reflectance in the disequilibrium compaction model. The model is calibrated with vitrinite reflectance data from Well E. The calibration in Well E is quite good. The model from vitrinite reflectance will also be used to determine the oil window, from which we can then determine the depth to the oil window.

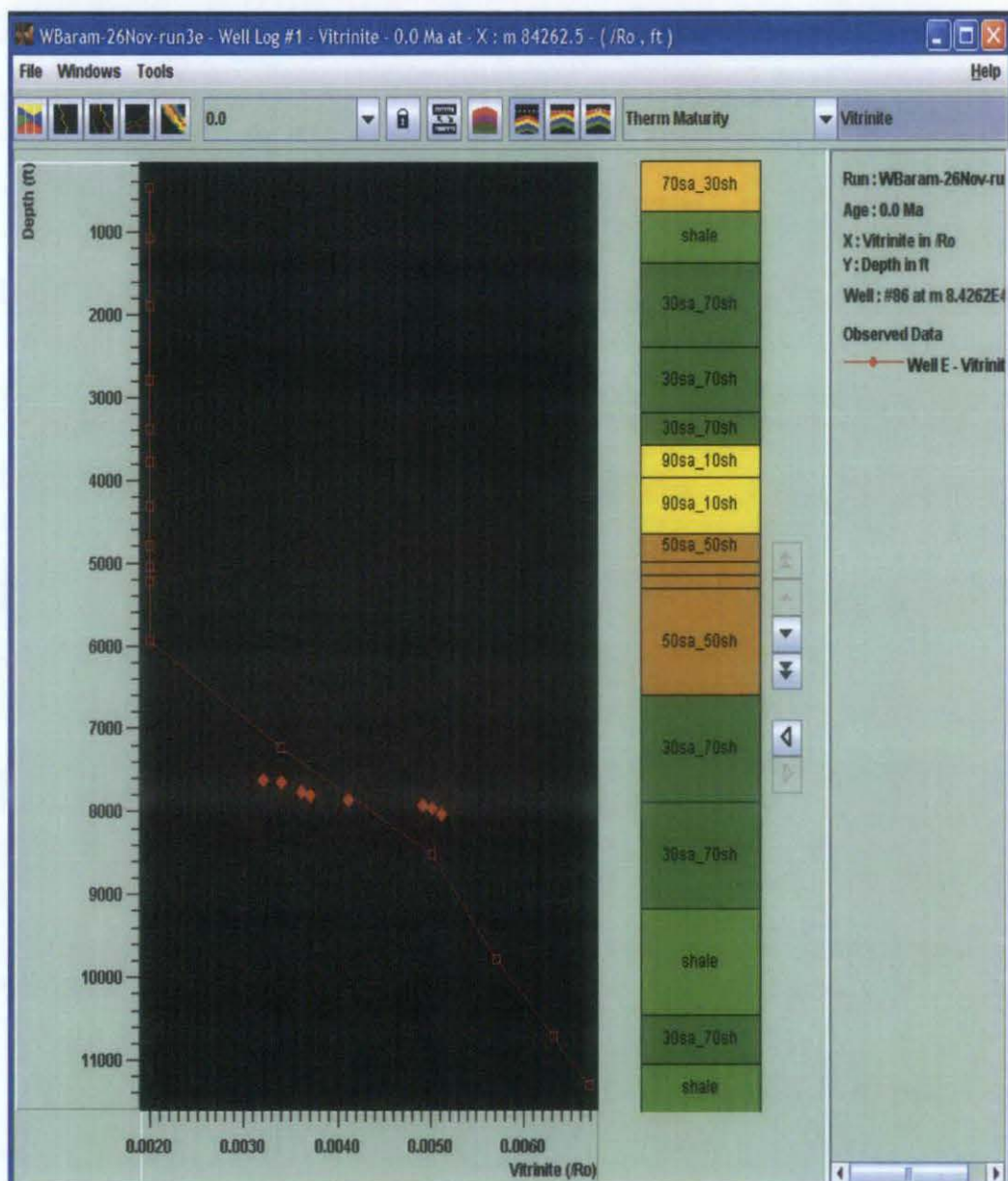


Fig. 4.36. The calibration of vitrinite reflectance in disequilibrium compaction model.

Figure 4.37 shows the modeled vitrinite reflectance along the section. The present day top of oil window generally occurs at depth approximately 10000 ft (3050 m). This is considering the cutoff of the oil window is 0.6 % Ro of the vitrinite reflectance.

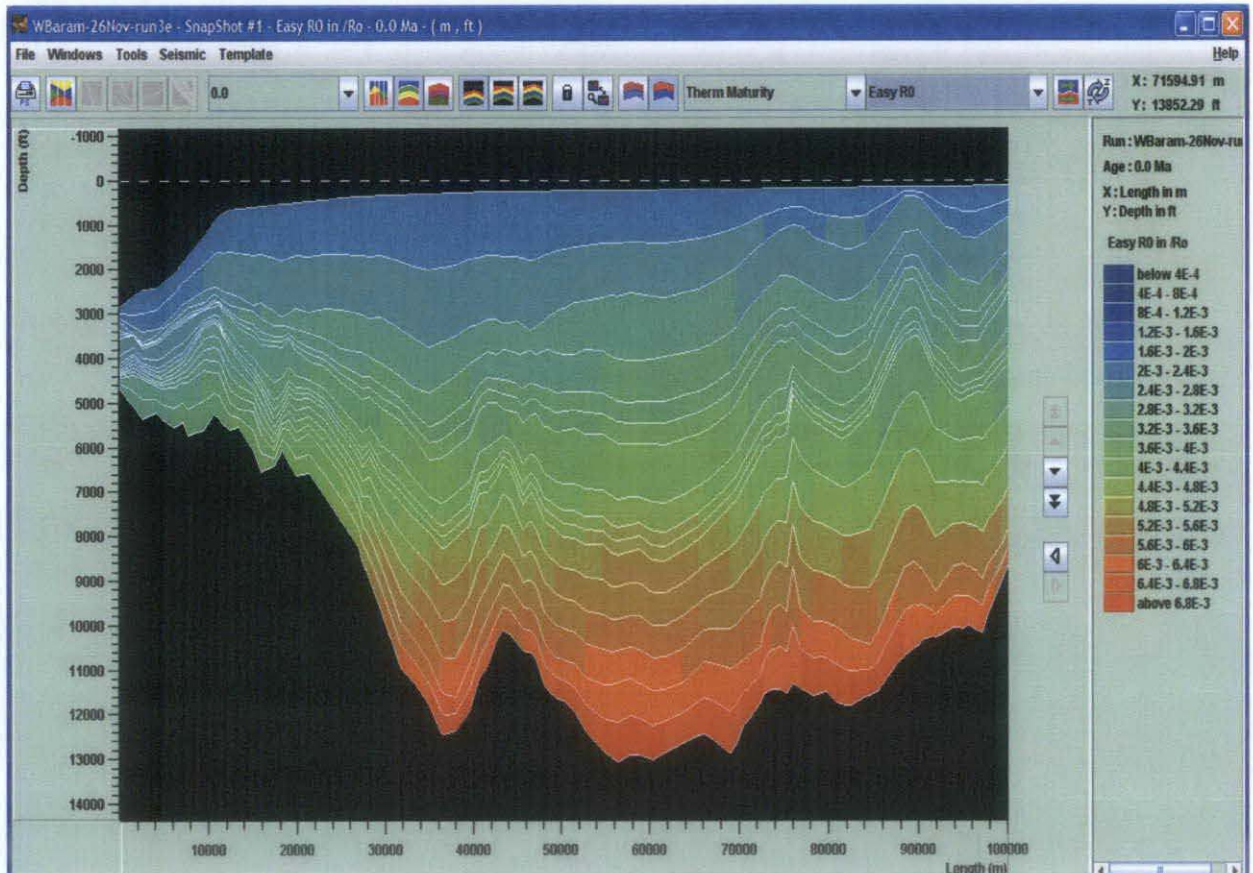


Fig. 4.37 the vitrinite reflectance model

From the temperature model (Figure 4.38), the temperature varies from 30-150°C. As the depth increases, the temperature also increases. Comparing the temperature model and the vitrinite reflectance model, it shows that when the depth increases, the value of the vitrinite reflectance also increases. In which this temperature will affect the thermal maturity of the kerogen. As mention before, the cut off of 0.6%Ro of the vitrinite reflectance marks the top of the oil window.

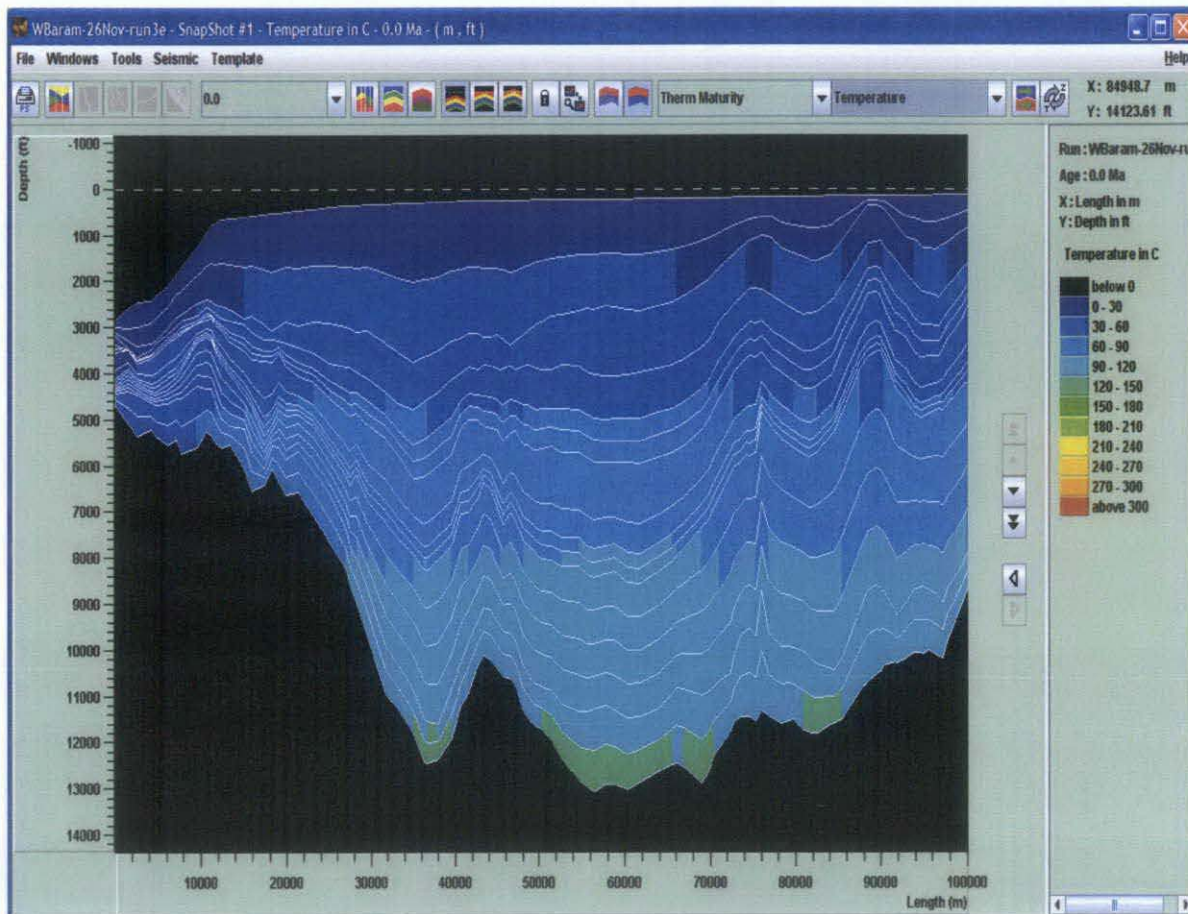


Fig. 4.38. The temperature model in present day for disequilibrium compaction.

Figure 4.39 shows the modeled overpressure distribution in the Baram Delta cross section. The onset overpressure is estimated at depth of 3050 m. Four wells were located on the seismic line from the model, the depth of overpressure for Well P, Well A4, Well O, and Well H are as below in table .The hydrostatic pressure gradient for the overpressure is 0.433 psi/ft. If the value of the pressure gradient is above this value, it is considered as overpressure. The overpressure predicted from the model is similar to the exact overpressure from the report (Table 4.5). This shows that the model of the overpressure is reliable.

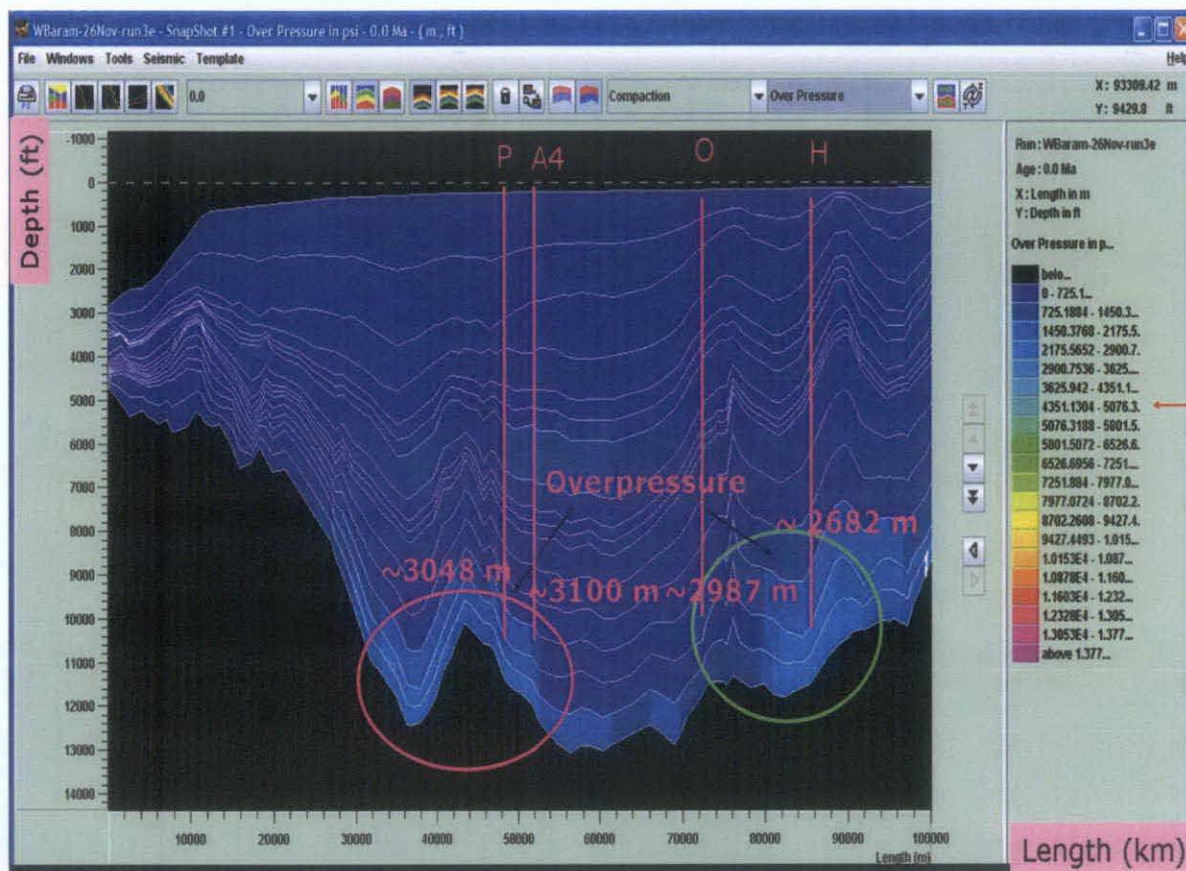


Fig. 4.39. The overpressure model for disequilibrium compaction

Table 4.5. The depth of overpressure from the model and from report.

Well	Depth of overpressure from model (m)	Depth of overpressure (m) (After PRSS research group unpublished report, 2006)
P	~3048	3021.952
A4	~3100	Not available
O	~2987	2959.14
H	~2682	2652.43

In the pore pressure estimation using Drillworks Predict the depth of the overpressure is much shallower than the actual top of overpressure in the report (The top of overpressure for Well H is 1000m and the top of overpressure for Well O is 1800m). This discrepancy is possibly related to incorrect normal compaction trend (NCT) or possibly due to the interbedded shale and sandstone, making it difficult to pick the clean shale. Since the top of overpressure in pore pressure estimation using Drillworks Predict is not really near to the actual top of overpressure, the 2D modeling is used to solve this problem.

## 4.5.2 Hydrocarbon Generation Model

Below is the construction of lithology model for hydrocarbon generation model (Figure 4.40). The present day top of oil window in West Baram Delta is 4000 m to 5000 m (Denis N. K. Tan et. al., 1999). In order to simulate the oil generation in the past, the depth of the section is added to 8000 m. Therefore, for this model, additional 4000 m of sediments is added. From the simulation of the model that includes hydrocarbon generation, the pressure model does not vary much from the first model (disequilibrium compaction). The overpressure model also does not vary much from the first model. Since the overpressure from the first and the second model does not vary much, it is likely that the origin of the overpressure in the West Baram Delta is due to disequilibrium compaction. Schreurs & Ellenor (1996) mentioned that rapid deposition of the fine-grained prodelta sediments can lead to the development of widespread overpressures generated by disequilibrium compaction. This overpressure within the prodelta shales is commonly associated with undercompaction and shale diapirism (Schreurs & Ellenor, 1996). Harrold et. al. (1999) also cited that the overpressure occurring in South East Asia is due to disequilibrium compaction. Kho et. al. (1994) also noted that the overpressure in Baram Delta can be due to shale diapirism.

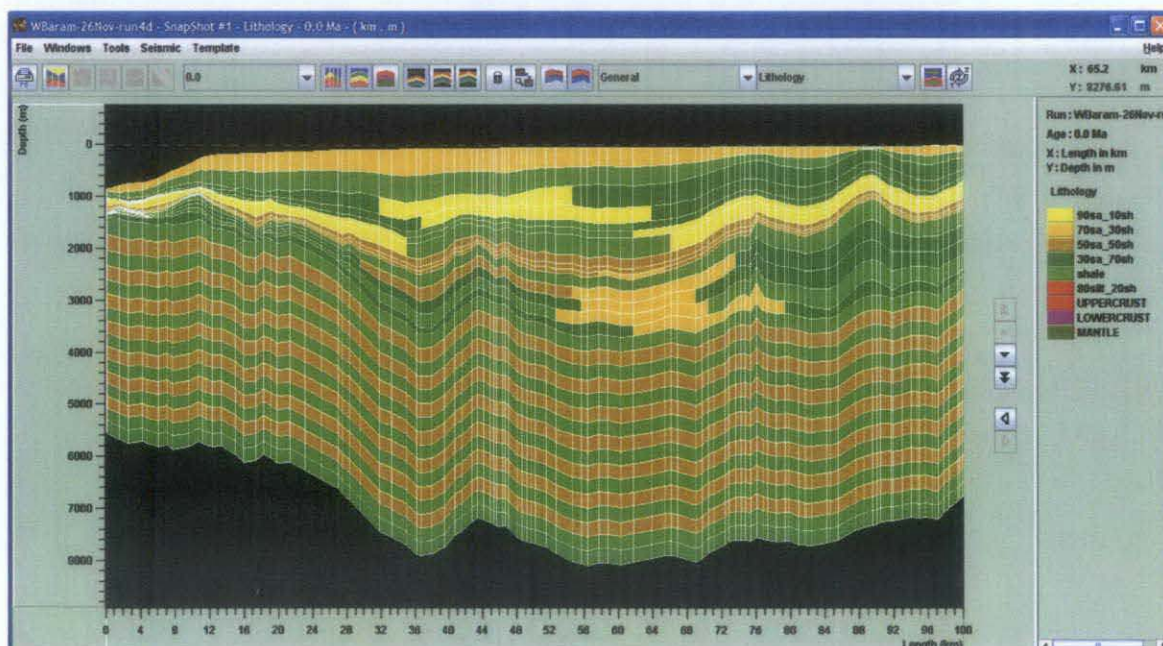


Fig. 4.40. The lithology model for hydrocarbon generation model.

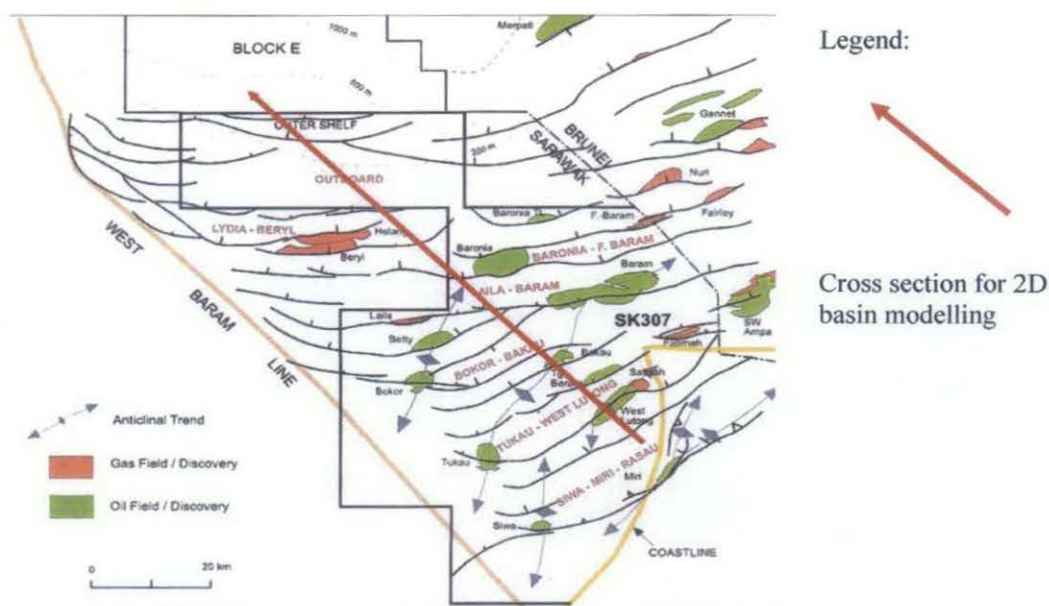


Fig. 4.41 West Baram major oil and gas fields (Adapted from Denis N. K. Tan et. al., 1999)

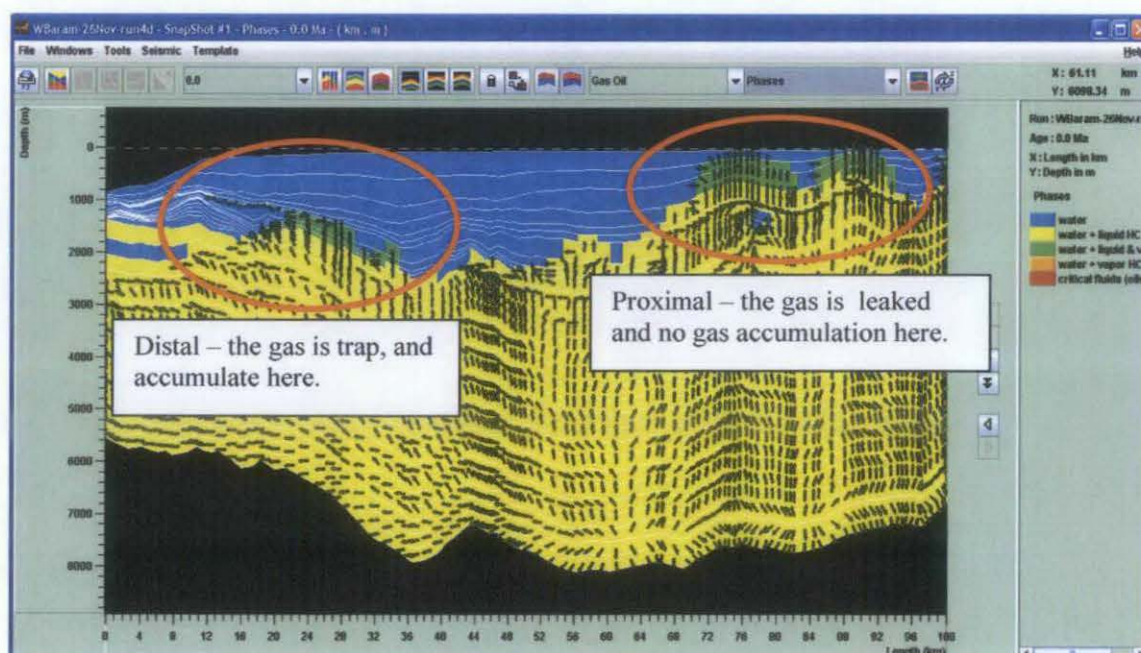


Fig. 4.42. The hydrocarbon expulsion for hydrocarbon generation model - hydrocarbon expulsion model.

Figure 4.41 show that there are many oil fields located in the proximal area, and many gas fields located on the distal area. This can be explained by the expulsion model from the basin modeling (Figure 4.42). In this model, it shows that in the proximal area, the gas evaporates and leaks; therefore, there are no gas accumulations (the gas is in green colour). In the distal area, the gas doesn't leak and traps, therefore, there are gas accumulations in this area

## CHAPTER FIVE

### 5.0 Conclusions and Recommendations

From this study, there are several conclusions:

- 1) In 1D (using Genex) the heatflow of the Baram Delta varies from 25 mW/m<sup>2</sup> to 55 mW/m<sup>2</sup> with the trend of the heatflow increases seaward. This is due to the high sedimentation rates in the proximal, and this will release the water in the pore. This will also lead to the quick dissipation of heat. The vitrinite reflectance data in this area is also not very reliable as the the vitrinite reflectance maybe suppressed and/or recycled.
- 2) In seismic interpretation (using Seiswork), we can see that the tectonics in the Baram Delta is very active as many growth fault can be seen. This high tectonism in Baram Delta leads to shale diapirism.
- 3) In pore pressure prediction (using Drillworks Predict), the top of overpressure for the well situated closer to the proximal, the top of overpressure occurs at shallower depths. This is due to the high sedimentation rates and rapid burial, creating an overpressure condition at shallower depth. For wells that are located near to the distal, the top of overpressure is occurs at deeper depths. This is due to the low sedimentation rates and the sediment is buried slowly.
- 4) In 2D basin modeling, the first model, which is the disequilibrium compaction, indicates that the depth to overpressure starts approximately at 3050 m (10000 ft). In the second model, which includes the hydrocarbon generation, the depth of overpressure does not seem to vary much from the first model. So, it is concluded that the main origin of overpressure in the West Baram Delta is disequilibrium compaction. Hydrocarbon generation does not contribute significantly to the development of overpressure in the West Baram Delta.



Below are several recommendations for this study to go far:

- 1) Better calibration can be done for the models if more and better data are available, such as temperature, vitrinite reflectance and pressure.
- 2) In order for this study to obtain a good end result, more time is needed than 4 months. Due to time constrain, the calibration of the data could not be very good.

## References:

- Abdul Jalil Muhammad & Azlina Anuar, (1999) Regional Petroleum Geochemistry of SK307 Baram Delta, Offshore Sarawak. Report. Petronas Research & Scientific Services Sdn. Bhd. Unpublished report.
- Azlina Anuar & Abdul Jalil Muhammad. 1999. Evidence for the origin of the West Baram Delta oils: Marine vs. Terrigenous. 21<sup>st</sup> Petroleum Geology Conference, Kuala Lumpur, Shangri-La Hotel, November 23-24, 1999. Poster.
- Azlina Anuar & Peter Abolins, (2005). Hydrocarbon charge modeling in deepwater NW Sabah, Msia. Poster. European Association of organic Geochemistry 22<sup>nd</sup> International meeting on organic geochemistry NH central conventions, Sevilla, Spain. 12-16 september, 2005.
- Bait, B. & Banda, R.M. 1994. Tertiary basins of North Sarawak Malaysia: a field excursion in the Tatau-Bintulu and Miri areas. AAPG International Conference and Exhibition, 21-24 August 1994.
- Bol, A.J. & Van Hoorn, B., 1980. Structural styles in Western Sabah offshore. Geological Society of Malaysia Bulletin 12, 1-16.
- Bruce, B. 2002. Pore Pressure Terminology. The Leading Edge.
- Denis N.K. Tan, Abdul Hadi B. Abd. Rahman, Azlina Anuar & Chow Kok Tho. 1999. West Baram Delta. The Petroleum Geology and Resources of Malaysia. Petroliam Nasional Berhad (PETRONAS). 293-342.
- Dickinson, G., 1953, Geological aspects of abnormal reservoir pressures in Gulf Coast, Louisiana: AAPG Bulletin, v. 37p. 410-432.
- Drillworks Pro Training Course, 2005. Knowledge Systems.

- Dutta N. C. 1987. Geopressure. Society of exploration Geophysics. United State of America: Society of Exploration Geophysicists.
- Ferguson, A. & McClay, K. 1997. Structural modelling within the Sanga PSC, Kutei Basin, Kalimantan: its application to paleochannel orientation studies and timing of hydrocarbon entrapment. Proceedings of the Petroleum Systems of SE Asia and Australasian Conference, May 1997, Indonesia Petroleum Association. 727–749.
- Harrold, T.W.D., R.E. Swarbrick, N.R.Goulty, 1999. Pore Pressure estimation from mudrock porosities in Tertiary basins, SE Asia, *AAPG Bulletin*, 83, p. 1057-1067.
- Ismail Che Mat Zin and Swarbrick, R.E., 1997. The tectonic evolution and associated sedimentation history of Sarawak Basin, eastern Malaysia: a guide for future hydrocarbon exploration. *In* Fraser, A.J., Matthews, S.J & Murphy, R.W., (Eds)., *Petroleum Geology of Southeast Asia*. Geological Society of London Special Publication, 126. 237-245.
- James, D.M.D. 1984. The Geology and Hydrocarbon Resources of Negara Brunei Darussalam. Special Publication, Muzium Brunei and Brunei Shell Petroleum Company Berhad.
- Kho, S.C., Hemmings, D. & Have, T.T., 1994. Overpressure in the Baram Field, offshore Sarawak, East Malaysia, *AAPG International Conference and exhibition*, Kuala Lumpur, Malaysia, August 21-24, 1994.
- Koopman, A., & James, D. M. D. 1996. Chapter 2. Regional Geological Setting. *In*, S. T. Sandal (Ed.), *The Geology and Hydrocarbon Resources of Negara Brunei Darussalam* (pp. 49–63). Bandar Seri Begawan: Syabas.

- Koopman, A., & James, D. M. D. 1996b. Chapter 3. Chapter 3 Structure. In S. T. Sandal (Ed.). *The geology and hydrocarbon resources of Negara Brunei Darussalam* (pp. 64–80). Syabas: Bandar Seri Begawan.
- Levell, B.K. 1987. The nature and significance of regional unconformities in the hydrocarbon-bearing Neogene sequences offshore West Sabah. *Geological Society of Malaysia Bulletin*, 21, 55–90.
- M Jamaal Bin Hoesni. 2004. *Origins of Overpressure in the Malay basin and its Influence on Petroleum Systems*. University of Durham.
- Mazlan B.Hj. Madon. 1999. Chapter 5. Basin Types. Tectono-stratigraphy Provinces, and Structural Style. *The petroleum Geology and Resources of Malaysia*. Petroliam Nasional Berhad (PETRONAS). pp 79-111.
- McClay, K., Dooley, T., Ferguson, A. & Poblet, J., 2000. Tectonic evolution of the Sanga Block, Mahakam Delta, Kalimantan, Indonesia. *AAPG Bulletin* 84, 765–786.
- Meissener, F.F., 1978a, Patterns of source rock maturity in non-marine source rock of some typical Western interior basins, in *Nonmarine Tertiary and Upper Cretaceous source rocks and the occurrence oil and gas in West-Central U.S.: Rocky Mountain Association of Geologist Continuing Education Lecture Series*, p.1-37.
- Meissner, F. F., 1978b, *Petroleum geology of the Bakken Formation, Williston Basin, North Dakota and Montana*, in 24<sup>th</sup> Annual Conference, Williston Basin Symposium: Montana Geological Society, .207-227.
- Morley, C.K., Back, S., Rensbergen, P.V., Crevello, P. & Lambiase, J.J. 2003 Characteristics of repeated, detached, Miocene–Pliocene tectonic inversion events, in a large delta province on an active margin, Brunei Darussalam, Borneo. *Journal of Structural Geology*, 25, 1147-1169.

- PRSS research group. 2006. The development of enhanced geophysical models for the prediction of deep reservoir. Unpublished report PRSS.
- Noor Azim Ibrahim, 1994. Major controls on the development of sedimentary sequences Sabah Basin, Northwest Borneo, Malaysia. Unpublished PhD Thesis, University of Cambridge, 254.
- Mohammad Yamin Ali, Wan Ismail Wan Yusof, Azlina Anuar, Idrus Mohd Shuhud, Mohd Fauzi Abdul Kadir & Md Nezam Mansor, 1995. Hydrocarbon prospectivity within and below the overpressured zone in Baram Delta province, offshore Sarawak. 109/90. Unpublished Research Project. Petronas Research & Scientific Services Sdn. Bhd.
- Morley, C.K., Crevello, P., Zulkifli, A., 1998. Shale tectonics-deformation associated with active diapirism: the Jerudong Anticline, Brunei Darussalam. *Journal of the Geological Society of London* 155, pp 475–490.
- Sandal, S.T. 1996. The Geology and Hydrocarbon Resources of Negara Brunei Darussalam (1996 revision). Brunei Shell Petroleum Company/ Brunei Museum. Bandar Seri Begawan: Syabas, Brunei Darussalam. 243 p.
- Schreurs, J., & Ellenor, D. W. 1996. The oil and gas resources of Brunei Darussalam hydrocarbon habitat. In, S. T. Sandal (Ed.), *The Geology and Hydrocarbon resources of Negara Brunei Darussalam* 147–154). Bandar Seri Begawan: Syabas.
- Swarbrick, R. E. and Osborne, M. J. 1998. Mechanism that generate abnormal pressure: an overview, *in* law, B. E., G.F. Ulmishek, and V.I Slavin eds., *Abnormal pressures in hydrocarbon environments: AAPG Memor* 70, p. 13-34.
- Tingay, M.R.P. Hillis, R.R. Morley, C.K, Swarbrick, R.E. & Okpere, E.C. (2002) Variation in vertical stress in the Baram Basin, Brunei: Tectonic and Geomechanical Implications. *Marine and Petroleum Geology*, 20, 1201-1212.

Zielinski, G.W., Bjorøy, M., Zielinski, R. L. B. & Ferriday, L. 2007. Heat flow and surface hydrocarbon on the Brunei continental margin: The American Association of Petroleum Geologists. 91: 1053-1080.

## Appendix 1: Well data

Wells	Geochemical data	Logs	Pressure	Temperature
Laila-1		√		
sidetrack-1	√	√		
sidetrack-2		√		
sidetrack-3		√		
Laila-2				
Merak-1	√			
Merak 2				
Merak 3				
Merak 4				
Betty 1		√	√	√
Betty - 1 sidetrack-1				
Betty - 1 sidetrack-2				
Betty - 1 sidetrack-3				
Betty-2			√	
Betty-3			√	
Betty-4			√	
Betty-5	√	√	√	
Betty-6		√	√	
Betty-6 sidetrack		√		
Betty-7		√		
Betty-8		√		
Betty-9		√		
Betty-11		√		
Betty-11 sdtr		√		
Betty-12 str		√		
Betty-13		√		
Betty-14		√		
Betty-15			√	
Betty-16			√	
Betty-17			√	
Bokor south-1	√		√	
Bokor-1		√	√	
Bokor-3			√	
Bokor-4	√		√	
Bokor-5			√	
Bokor-6			√	
Bokor-7			√	
Bokor-8		√		
Hasnah-1	√	√	√	√
Bakau deep-1	√	√	√	√
Bakau-1			√	
Bakau-2			√	
Tukau Timur-2		√		
Tukau-1				
Tukau-2	√	√		√
Tukau-3				

Wells	Geochemical data	Logs	Pressure	Temperature
Tukau-4		√		
Tukau-5		√		
Tukau-6				
Tukau-7				
Tukau-8				
Tukau-9		√		
Tukau-10		√		
Tukau-11		√		
Tukau-12		√		
Tukau-13		√		
Tukau-42	√			
Sikau North-1		√		
Sikau-1				
Sikau-2		√		
Loak Bay		√		
Loak bay 604				
loak bay 610				
Siwa-1				
Siwa2		√		
Siwa-3		√		
Siwa-4	√	√		√
Siwa-5		√		
Midin-1				
Baronia timur laut-1	√	√	√	
Baronia barat-1	√	√		√
Baronia-1	√	√		
Baronia-2		√		
Baronia-3		√		
Baronia-4				
Baronia-5				
Baronia-11				
Baronia-19				
Baronia-46				
Baronia-29	√			
Faridah -1		√		
Faridah-23				
Fairley Baram-1			√	
Fairley Baram-2			√	
Fairley Baram-3	√	√	√	√
Fairley Baram-11			√	
Fairley Baram-29			√	
Baram-1			√	
Baram-2	√		√	
Baram-3			√	
Baram-4			√	
Baram-5			√	
Baram-6			√	



Wells	Geochemical data	Logs	Pressure	Temperature
Baram-7	√		√	√
Baram-8			√	
Baram-16			√	
Baram-20		√		
Baram-21		√		
Baram-23		√	√	
Baram-24				
Baram-25				
Baram-26		√		
Baram-27				
Baram-28		√		
Baram-32			√	
Baram-41			√	
Baram-42			√	
Baram-43				
Baram-44			√	
Baram-55			√	
Baram-56				
Baram-59			√	
Fatimah -1		√		
Tanjung Baram-1	√		√	
Kuala Baram-1	√			
West Lutong-1	√			√
West Lutong-2				
West Luotong-3				
West Lutong-4				
West Lutong-5				
Zarina-1	√	√	√	
Sikap-1	√	√		
Layang-1	√	√	√	√
Beryl-1	√		√	
Beryl-3	√	√	√	
Beryl-4		√	√	
Beryl-5		√	√	
Beryl-6		√	√	
Beryl-7		√	√	
Lembuk-1	√			√
Lembuk-2				
Lembuk-3			√	
Lembuk-4			√	
Lembuk-5			√	
Lembuk-6			√	